Improving Geological Saline Reservoir Integrity through Applied Mineral Carbonation Engineering

Dissertation submitted in partial fulfilment of the requirements of the University of Pretoria for the degree of Master of Science

By

Thembane Kelvin Mlambo

Department of Geology,
University of Pretoria (South Africa)

March 2012

ABSTRACT

The most widely advocated method of carbon capture and storage involves the injection of CO_2 into underground geological formations. Key to the development of this geological sequestration technology is the existence of suitable high-integrity geological sites for the safe, long-term storage of CO_2. Unlike depleted oil and gas reservoirs which are historically proven to be well-defined, formations with saline brines may not have a similar proven sealing capacity. In the main, complex geochemical reactions occur in the supercritical CO_2 / brine / host rock environment which can cause significant changes in the porosity, permeability and injectivity of the formation. Depending of the nature of the processes, the effects of the underground injection of CO_2 may (1) yield increased storage capacity of the target horizon, or (2) lead to increased potential for leakage beyond the confining layers of the saline formation, or (3) impede the injection exercise as a whole. It is conceivable that accelerated, localized mineral carbonation could be induced at strategic places between the CO_2 plume and fault zones or facies changes present in deep saline formations, in order to prevent the migration of CO_2 outside the confined layers of the reservoir.

The South African electricity producer, Eskom, generated 36.01 million tons of coal-combustion fly ash in 2010. About 5.6% were reused for the production of cement. The remaining 33.89 million tons were safely disposed of and managed on Eskom ash dumps and dams which are located adjacent to their corresponding power stations. South Africa has a long history regarding the development of new applications for this material and is very active in the development of ash technologies. Concurrently, the power industry is also a major carbon dioxide (CO_2) emitter, with Eskom's emissions approximating 225 million tons for 2010.

In this study, the author introduces a theoretical concept whereby fly ash in a slurry form could be injected at strategic sites of deep saline formations. The purpose of this injection strategy is to prevent the migration of injected anthropogenic CO_2 plumes beyond the confining layers of the formations, via induced *in situ* localized, accelerated mineral carbonation. The proposed application falls within the carbon capture and storage (CCS) initiative by geological sequestration and aims at improving the integrity of deep saline formations which may be at risk of leakage upon injection of CO_2.

The use of coal-combustion fly ash in industrial mineral carbonation and the research involving its applications in carbon capture and storage (CCS) has internationally gained increased attention. However, the work involving fly ash in industrial mineral carbonation has only focused on the sequestration of sub-critical CO_2.

This work demonstrates for the first time that fly ash can react with supercritical CO_2 under varying pressure and temperature conditions. The experiments were conducted following an assumed geothermal gradient for deep saline reservoirs, as described by Viljoen, 2010, i.e. 44˚C/80bar and 50˚C/100bar. Ultra-pure water was used as a solvent. The duration of experiments ranged from 60 minutes to 7 days. Under these T/ P conditions, carbonates in the form of calcite ($CaCO_3$) were only detected at completion of the 7 days experiment.

Further investigation was undertaken at 90˚C/90bar for 2 hours using synthetic brine as a solvent, in order to mimic the composition of deep saline formations. This work yielded both aragonite and calcite, which formed as sheets at the base and on the walls of the batch reactor. The carbonated sheet fragments were examined using scanning electron microscopy (SEM) and were found to have an approximate thickness of 16 µm. A thinner layer of white precipitate on the walls of the reactor was composed of aragonite and calcite and contained an amorphous phase of carbonate of *ca.* 1% by volume. The mineralogical composition of these carbonated sheets was confirmed using XRD, which demonstrated the presence of aragonite (23%), calcite (3%) and fly ash minerals (*e.g.* mullite, quartz). It also contained an XRD-amorphous phase of about 37%. These sheets were thus enriched in calcium and carbon but also other elements were found to be present (Al, Si, Na, Mg and Cl) as shown by SEM. It is, however, unclear whether these elements identified in the spectrum are part of the sheet or are rather indicative of an effect of analytical volume created by the SEM electron beam being larger than the thickness of the sheet. Small amounts of S were also detected. Fly ash particles as well as a small number of needle-shaped gypsum crystals were visibly embedded in the sheet (SEM).

ACKNOWLEDGMENTS

Thanks to Council for Geoscience particularly Dr. Marthinus Cloete for hosting me through my internship and for this great opportunity to be involved in this study. To the Mining Qualification Authority (MQA), NRF and South African Centre for Carbon Capture and Storage (SACCCS) thanks for financial support. I would like to thank IEAGHG for the training they provided on CCS fields. Thanks to Dr. Richard Kruger and Petroleum Agency SA (PASA) for providing me with fly ash samples and sandstone samples, respectively. Thanks to Ms Corlien Cloete, Ms Maria Atanasova and Ms Hilda Cronwright for the help with analytical techniques. Last but not least, many thanks to Dr. Frederic Doucet, Dr. Elizabet M. van der Merwe and Prof. Wladyslaw Altermann for their incredibly supervision, mentorship, support and mostly importantly for believing in me.

ACADEMIC OUTPUTS

Annual Technical Reports:

T.K. Mlambo, F.J. Doucet, E.M. van der Merwe, W. Altermann, Maria Atanasova, and Richard A. Kruger, (2011). Improving Geological Saline Reservoir Integrity through Applied Mineral Carbonation Engineering, Annual Progress Report No (2011-0050), Council for Geoscience.

Frédéric J. Doucet and **Thembane K. Mlambo**, (2010). Development and optimization of steel slag reprocessing technologies with implications for the steel and cement manufacturing sectors and for long-term CO_2 sequestration, Annual Progress Report: 2009-0037, Council for Geoscience.

Conference Proceedings:

T.K. Mlambo, F.J. Doucet, E.M. van der Merwe, W. Altermann, Maria Atanasova, and Richard A. Kruger, (2011). Improving Geological Saline Reservoir Integrity through Applied Mineral Carbonation Engineering, Second South African CCS Week, Midrand, South Africa, 24-28 October.

T.K. Mlambo, F.J. Doucet, E.M. van der Merwe, W. Altermann (2011). Improving CO_2 confinement in deep saline formations via induced carbon mineralization. Abstract Book of GeoSynthesis 2011, Abstract No 74.

T.K. Mlambo, F.J. Doucet, E.M. van der Merwe, W. Altermann, M. Atanasova, R.A. Kruger (2011). Sequestration of Supercritical CO_2 in Coal Fly Ash, Proceedings of 2011 Underground Coal Gasification (UCG), Sandton, South Africa, 13-14 July.

T.K. Mlambo, F.J. Doucet, E.M. van der Merwe, W. Altermann, M. Atanasova, R.A. Kruger (2011). The injection of fly ash slurries in deep geological reservoirs for improved reservoir integrity and safe CO_2 sequestration. Proceedings of the 2011 World of Coal Ash Conference, Denver, Colorado, USA, 9-12 May.

T.K. Mlambo, F.J. Doucet, E.M. van der Merwe, W. Altermann (2011). Conceptual approach to CO_2 mitigation: Applying chemical carbonate mineralization principles to geological CO_2 sequestration. 40th South African Chemical Institute Convention (SACI), Johannesburg, South Africa, 16-21 Jan.

T.K. Mlambo, F.J. Doucet, E.M. van der Merwe, W. Altermann (2011). CO_2 geological sequestration: Improved reservoir integrity via carbonation. oral presentation at the 23rd Colloquium of African Geology, Johannesburg, South Africa, 8-14 Jan.

T.K. Mlambo, F.J. Doucet, E.M. van der Merwe, W. Altermann (2010). The application of mineral carbonation engineering principles to geological CO_2 sequestration: A conceptual approach to improved reservoir integrity. In: Proceedings of Accelerated Carbonation for Environmental and Materials Engineering conference, Turku, Finland, 29 Nov - 1 Dec.

TABLE OF CONTENTS

FIGURES

TABLES

LIST OF ABBREVIATIONS

ARC	Albany Research Center
BET	Brunauer, Emmett and Teller Theory
C&S	Carbon and Sulphur
CCS	Carbon Capture and Storage
CCSP-H1	U.S. Climate Change Science Program
CDM	Clean Development Mechanisms
CFC	Chlorofluorocarbon
CGS	Council for Geoscience
CSIR	Council for Scientific and Industrial Research
CTL	Coal to Liquid
CO_2	Carbon dioxide
COP	Conference of People
CSLF	Carbon Sequestration Leadership Forum
EIA	U.S. Energy Information Administration
EAR	Eskom Annual Report
GHG	Green House Gas
ICCS	Introduction to Carbon Capture and Storage workshop notes
ICP-MS	Inductive Couple Plasma Mass Spectroscopy
IEA	International Energy Agency
IEAGHG	International Energy Agency GHG
IPCC	Intergovernmental Panel on Climate Change
LOI	Loss on Ignition
$NaHCO_3$	Sodium bicarbonate
NASA	National Aeronautics and Space Administration
NETL	National Energy Technology Laboratory
PASA	Petroleum Agency SA
PDS	Particle Size Distribution
sc-CO_2	Supercritical CO_2
SACCCS	South African Center for Carbon Capture and Storage
SEM	Scanning Electron Microscopy
S:L	Solid Liquid Ratio

T/P	Temperature/pressure
TNO	Netherlands Organisation for Applied Scientific Research
UNFCCC	United Nations Framework Convention on Climate Change
WMO	World Meteorological Organization
WP	Work Package
wt %	Weight Percentage
WWF	World Wildlife Fund
XRD	X-ray Diffraction
XRF	X-ray Fluorescence

CHAPTER ONE
INTRODUCTION

1.1 Background

Since the beginning of the Industrialisation (1750) the concentrations of carbon dioxide (CO_2) (measured in ice core) in the atmosphere has increased by about 39% from 280 to 389 ppm (WMO, 2011). The increase of CO_2 in the atmosphere is mostly associated with fossil fuel combustion, deforestation and land-use change. The annual average growth rate of CO_2 content in the atmosphere was 35.7% from 1990 to 2005, exceeding the average increase from 1960 to 2005 of 26.3% (di Norcia, 2008). If the current CO_2 emission rate continues, the atmospheric CO_2 will increase to more than double the amount of the pre-industrial period by 2070, and 8 times that by the year 2300 (Hay, 2011). This brings about concerns since higher concentrations of greenhouse gases (GHG), particularly CO_2 (750 ppm), are associated with the warmer earth during Cretaceous and Eocene (DeConto et al. 2008). According to Court (2011) atmospheric CO_2 concentrations need to be kept below 450 ppm, to avoid climate-tipping elements and unmanageable changes.

In addition, CO_2 contribution to the overall global radiative forcing is showing an increase from 62% in 2006 to 64% in 2011 (WMO, 2006 and 2011). Radiative forcing is defined by IPCC, 2007 as *"the change in net irradiance at the tropopause after allowing for stratospheric temperatures to readjust to radiative equilibrium, but with surface and tropospheric temperatures and state held fixed at the unperturbed values."* Furthermore, CO_2 is responsible for 85% and 83% of radiative forcing over the past decade and over the last five years, respectively (WMO, 2010).

Other important GHGs include methane, nitrous oxide, CFC-12 and CFC-11. These GHGs are regarded as the most important ones because their contribution to global warming or climate change is significant. Such gases have a long lifetime that allows them to spread widely and evenly across the atmosphere (NASA, 2005). According to WMO (2010) these GHGs, with CO_2 included, are responsible for about 96% of the increase in radiative forcing due to long-lived greenhouse that has occurred since 1750. However, methane is showing a gradual decrease in its total global radiative forcing contribution from 20% in 2006 to 18% in

2011, whereas, the global radiative forcing for nitrous oxide has been fairly constant at 6% over the past seven years (WMO, 2006 and 2011).

Research has shown that the most important green house gases (GHGs) are CO_2 and methane, with methane being about 21 times more potent than CO_2. The concentration of methane has more than doubled in the last two centuries, but has remained fairly low (~1755 ppb) in the atmosphere (CCSP-H1, 2006). It also reflects a relatively positive development with respect to its atmospheric concentration over the past two decades. The overall methane growth rate had slowed down from 1984 to 1999 (Dlugokencky et al., 2003) and the concentration of methane in the atmosphere had not increased between 1999 and 2006 (Dlugokencky et al., 2009).

Nitrous oxide, through chemical reactions known as fostering, can reduce the concentration of methane and thereby contribute to climate change mitigation (NASA, 2005). It can also be removed from the stratosphere through photochemical processes (WMO, 2010). Ozone is produced by chemical reaction involving GHGs such as carbon monoxide, nitrogen oxides and methane. Therefore, the ozone concentration can be reduced by reducing the concentration of these GHGs.

The concentration of methane, nitrous oxide, CFC-12, CFC-11 and ozone are negligibly low or showing a gradual decrease in more recent years. Ozone can be controlled by minimising the precursors. But CO_2 concentrations are increasing at an alarming rate, thus posing a threat to the environment.

1.2 CO_2 Mitigation

The Kyoto Protocol is one of the most noticeable international actions against the increase of CO_2 emissions. It was developed under United Nations Framework Convention on Climate Change (UNFCCC) during the Conference Of Parties 7 (COP7), held in Kyoto, Japan, December 1997. This is an agreement that legally binds all Annex-1 parties (developed countries) to collectively reduce their GHG emissions by 5.2% compared to their 1990 emissions, from 2008 to 2012. Though this is a collective target, each country was assigned a certain percentage of emission reductions to reach this target.

This target is to be achieved by all parties through emission trading, joint implementation and/or clean development mechanisms (CDM). In a nutshell, emission trading is a form of carbon trading that permits Annex-1 countries that have excess carbon credits to sell them to other Annex-1 countries. Joint implementation allows Annex-1 country to invest in a "carbon-mitigation" project from another Annex-1 country to earn carbon credits. Lastly, CDM permits Annex-1 country to invest in a "carbon-mitigation" initiative in Non-Annex-1 country (developing countries) to earn carbon credits.

However, this target is only achievable if carbon management techniques are implemented holistically. Basically, these are policies and techniques introduced to reduce carbon emissions namely energy efficiency, reduction of energy demands, the use of carbon free energy sources and carbon capture and storage (CCS) (Kaszuba et al., 2003).

Initially, CCS was not included in CDM until in COP17, held in Durban, South Africa, December 2011. CCS is regarded by IEA as the most effective means of reducing CO_2. According to IEA (2010), CCS will contribute up to 31% in the reduction of international CO_2 emissions. However, in this case CCS only refers to geological sequestration, which is mostly referred to as CCS, see Chapter 2.

1.3 South African Perspective

Non-Annex-1 parties do not have a specified level of CO_2 emission reduction, because the current global CO_2 concentration is thought to be brought about mainly as a result of emissions from Annex-1 countries. This does not, however, exempt Non-Annex-1 countries from reducing their GHG emissions. Since this situation is steadily changing, especially now that the developing countries are among the top emitters in the world with China at the top of the list and South Africa taking 13th place (reported as Total Emissions**,** Million Metric Tonnes of CO_2 per annum) (EIA, 2008).

About 93% of South Africa's electricity is generated from coal, while the other 7% is generated from nuclear, solar and wind harvesting. Coal provides 73% of South Africa's primary energy and Sasol's coal-to-liquid (CTL) technology provides half of South Africa's fuel (Eberhard, 2011). The South African fossil fuel energy industry emits more than 40% of Africa's fossil fuel-related CO_2 and about 1% of the world's total emission. The total South African CO_2 emissions are currently at about 500 million tonnes per annum, but only 320

million tonnes of CO_2 is produced at the fixed-point sources (i.e. power stations, coal-to-liquid plants etc) (Viljoen, 2010). This figure is expected to increase to 441 million tonnes per annum in the near future (Viljoen, 2010).

The on-growing energy demands have compelled Eskom to build two new coal-fired power stations namely the 4764 MW Medupi plant and the 4800 MW Kusile plant (Eberhard, 2011). More coal power plants and CTL plants are anticipated in the near future from Eskom and Sasol, respectively. Therefore, CO_2 emissions are expected to continue to increase for the next 24 years (until 2025). Thereafter, CO_2 emissions will be regulated such that the emissions are capped (ideally) for about 10 years (2025-2035), after which it will start to decrease (WWF, 2011).

1.4 South African Carbon Sequestration Initiative

Since the adoption of the Kyoto Protocol in 1997, the international community has shown great response with regard to climate change abatement, and South Africa is no exception. The establishment of the South African Centre for Carbon Capture and Storage (SACCCS) that oversees all the CCS events and initiatives of the country, demonstrates South Africa's endeavour towards CO_2 mitigation. The CCS Potential in South Africa and the Atlas on Geological Storage of Carbon Dioxide in South Africa were published in 2004 and 2010, respectively, see the South African CCS roadmap (Figure 1.1). The scoping study on mineral carbonation was published in 2011 (see below). Currently, the SACCCS is preparing for the test injection, due in 2016.

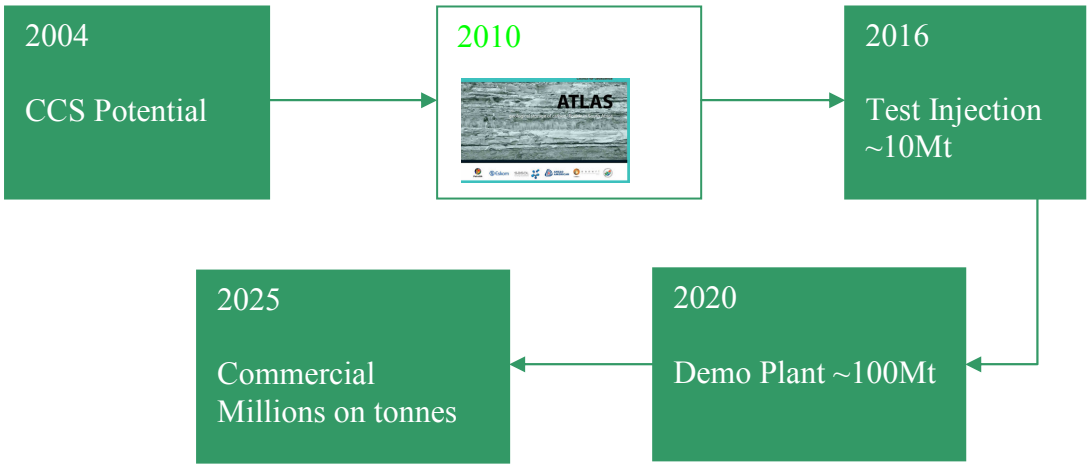

Figure 1.1: South African carbon capture and storage roadmap

The CCS Potential study was the first work done on CCS in South Africa. This investigation was undertaken by the Council for Scientific and Industrial Research (CSIR) for the then Department of Minerals and Energy, to evaluate and assess in a broader perspective of implementing CCS in South Africa (Engelbrecht, 2004). Several CO_2 mitigation technologies were recommended (i.e. biological sequestration, geological sequestration and marine sequestration), which are still under investigation.

In view of the findings of this initial report, South Africa followed up with the compilation of the atlas (Atlas on Geological Storage of Carbon Dioxide in South Africa, Cloete, 2010). This was a desk-top study set to identify potential storage sites (i.e. saline formations and depleted oil and gas reservoirs), including their capacity estimates. The Atlas reported the theoretical storage capacity of CO_2 in South Africa to be about 150 Gt. The largest storage capacity of about 98% is offered by the offshore Mesozoic basins: Orange, Outeniqua and Durban/Zululand; as illustrated in Figure 1.2 (Cloete, 2010). The identification of these basins created some concerns with regard to geological storage in South Africa. The distance between the point sources and the storage sites is fairly large and the reservoirs are mostly offshore, which could increase the cost of transportation (see section 2.4). Another challenge faced by the South African CCS industry is the lack of world class storage sites. The considered saline reservoirs have low integrity (fractures) that may provide CO_2 a pathway to the surface (see section 2.1.2).

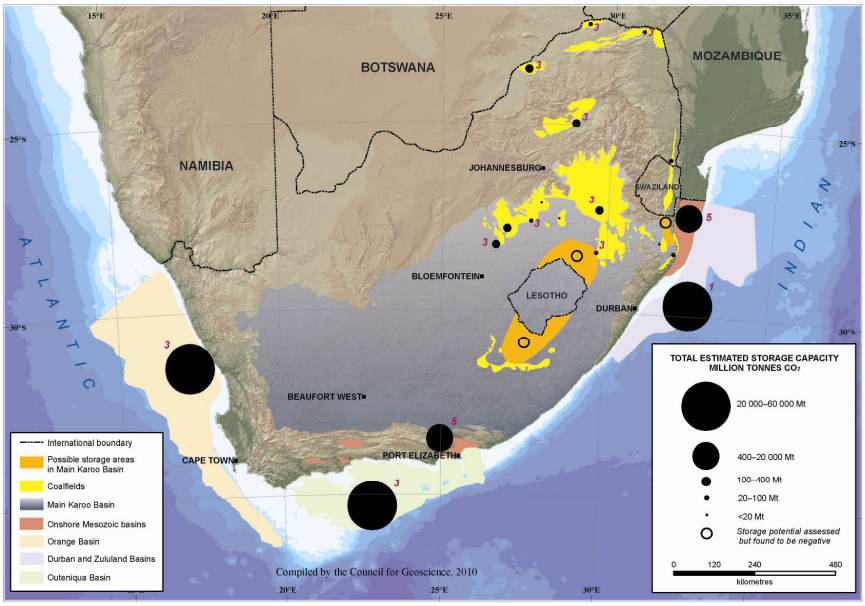

Figure 1.2: Map showing the Orange, Outeniqua and Durban/Zululand basins and estimated CO_2 storage capacities of geological storage in South Africa (Cloete, 2010)**. The storage capacities are illustrated with black shaded circles**

The Scoping Study on Mineral Carbonation Technologies, (Doucet, 2011), is another carbon mitigation option which falls under the umbrella of CCS, but which is not included in the existing SACCCS roadmap, was commissioned by SACCCS in 2010 to Council for Geoscience (CGS). This study looked at the possibility of using various materials such as mine tailings, steel furnace slag, phosphogypsum and coal-combustion fly ash for CO_2 sequestration.

1.5. Theoretical Concept

This project is set to feed into the development of CCS in South Africa and the accomplishment of the aforementioned targets. South Africa only possesses few small oil and gas reservoirs. Therefore, saline formations will be the main form of geological CO_2 sequestration. However, saline reservoirs do not have a proven sealing capacity that can match the oil and gas reservoirs. Depleted oil and gas reservoirs are historically proven to be well-confined. These saline reservoirs are rarely isolated and possess some level of recharge, flow and discharge. These movements are likely to increase porosity and permeability of the formation that could increase the CO_2 leakage potential. Hence, this work looks into one of the options that could act as an important risk mitigation strategy for CO_2 storage in saline formations.

1.6. Problem Statement

Saline reservoirs may not have a proven sealing capacity and increase in porosity and permeability due to aggressive supercritical (sc) CO_2/brine mixtures has been reported, which could cause increased risk of leakage beyond the confining layers.

1.7. Objectives

Objective 1: To present and discuss a theoretical concept and strategic injection, that could be used to improve the integrity of deep saline formations for long-term CO_2 storage. This concept could be accomplished by injecting mineral slurries and thereby creating mineral and carbonate curtains for better CO_2 containment.

Objective 2: To demonstrate that coal-combustion fly ash does react with CO_2 in a brine environment under sc-CO_2 conditions.

1.8. Research Approach

Theoretical scenarios, first developed by Rush and O'Connor (2005), were adopted to fit within the scope of this project. These scenarios are presented in details in Chapter 3. This was followed by identification of materials that can be used in mineral carbonation and that could be used for improving saline reservoir integrity. The proposed materials were steel furnace slag, ultramafic minerals or fly ash. The latter was regarded to be the best candidate because it is abundant and readily available at low cost, is generally much more reactive than primary minerals, has good rheology and can provide calcium (Ca) and magnesium (Mg) ions to accelerate the precipitation of CO_2 as mineral carbonates (section 3.1). This material was then characterized using various analytical techniques.

Thereafter, the average chemical composition of deep saline brine was obtained from international literature. The South African saline brine chemical composition was unavailable. Then carbonation experiments were designed with respect to temperature/pressure (T/P) conditions present in deep saline reservoirs, as well as, with respect to solid/liquid (S/L) ratio for the best carbonate yield.

1.8.1 Hypotheses

Hypothesis 1: Supercritical CO_2 can react with a synthetic saline brine to form stable mineral carbonates when the pH is adjusted to above 8 by adding sodium hydroxide (NaOH).

Hypothesis 2: Coal-combustion fly ash can be used to increase the pH of the saline brine solution instead of NaOH. Then the fly ash/brine mixture can react with sc-CO_2 of varying densities to form stable mineral carbonates.

Hypothesis 3: The carbonation reaction concept stated in Hypothesis 2 can be used to accelerate mineral carbonation in sandstone cores, sampled from saline reservoirs, and decrease aggressive dissolution behaviour of sc-CO_2/brine mixtures.

CHAPTER TWO
LITERATURE REVIEW

2.1 Carbon Capture and Storage (CCS)

CCS is an integrated carbon mitigation technology, which consists of three major stages: capturing CO_2 from fixed-point sources, transport to a storage site and the storage. Each of these stages will be discussed in more details in the sections below. CCS is often used synonymously to geological CO_2 storage, whereas, CCS actually refers to all technologies which consist of the three aforementioned stages e.g. ocean storage, as mineral carbonates, or for use in industrial processes (IPCC, 2005).

2.1.1 Capture

In CCS, "capture" refers to the process where CO_2 is separated from other flue gases (e.g. NOx, SO_2 combustion resistant particles, etc.) to produce a concentrated stream of CO_2. This process is essential since flue gas from coal power station typically contains between 7 and 14% CO_2. However, a CO_2 stream with purity above 90% is required in order to optimise the storage capacity and to prevent corrosion in the pipeline (section 2.1.2). This phase is the most expensive, and is estimated to contribute about 75% of the total CCS operational costs (Knauss, 2003). The purification technology is, nonetheless, progressing faster and seems to be well advanced when compared to the storage phase (IEAGHG, 2010). This process can be undertaken by techniques including pre-combustion, post-combustion and oxyfuel combustion capture (Figure 2.1).

The Coal-to-Fuel (CTL) technology is highly favoured in CCS because it produces CO_2 of high purity, thus eliminating significant cost of capture. For example, Sasol's CTL plant produces annually about 32 million tonnes of a 90-98% pure CO_2 stream. Some form of minor scrubbing may be required depending on the types of impurities and the pipeline material (section 2.1.2).

A pre-combustion process captures CO_2 prior to combustion, by reacting fuel with air or oxygen to produce a fuel that contains CO and H_2. This fuel is then reacted with steam to produce a mixture of CO_2 and H_2.

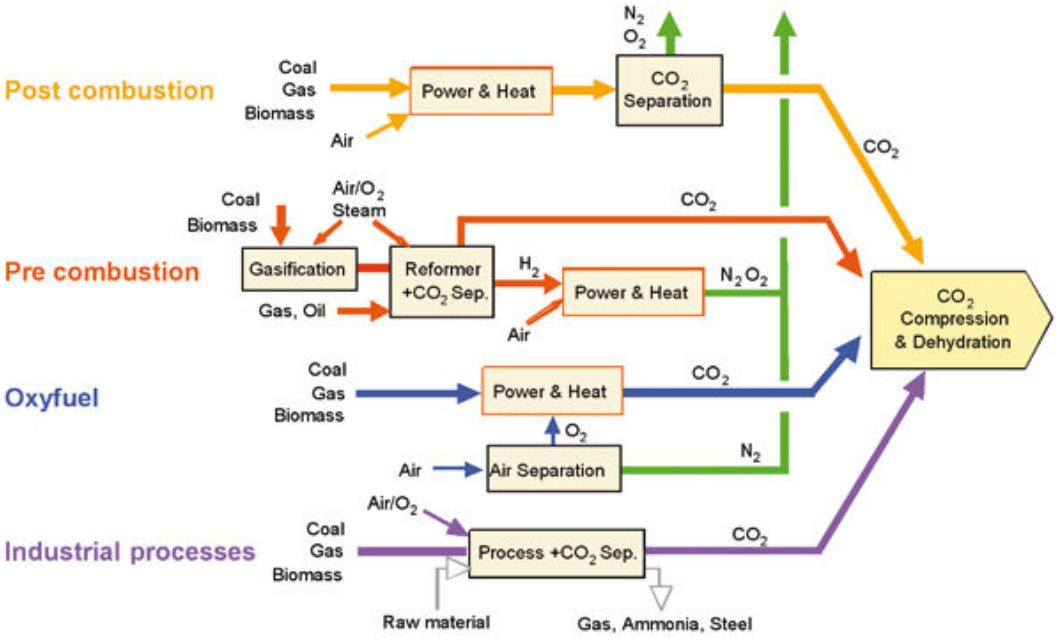

Figure 2.1: Different techniques and steps involved in CO_2 capture processes (IPCC, 2005).

The post-combustion capture process is used to separate CO_2 from the rest of the flue gases along the product-processing stream from combustor to effluent exhaust. It yields about 15% mole fraction of CO_2 (IEAGHG, 2008). This capture process mostly uses absorption solvents i.e. amine or ammonia. However, using amines as a solvent possesses a challenge because it reacts with NOx and SOx to form stable salts (IEAGHG, 2008). Therefore, NOx and SOx needs to be removed prior to scrubbing. The adsorption solvents (zeolites) and membranes are barely used because there are still on the development stage.

Oxy-combustion capture is achievable by burning fossil fuel with nearly pure oxygen. This process produces a flue gas rich in CO_2 while water vapour gets separated by condensation.

2.1.2 Transport

The most efficient means of transporting CO_2 is by pipeline in the gas and/or liquid phase. It is possible to transport CO_2 in solid form but the process is very energy intensive. Pipeline systems are the most favoured means of CO_2 transportation because it is a well known technology, safe, low cost, energy efficiency, and can deliver a steady and constant supply

(CSLF, 2011). This type of system can run up to thousands of kilometers. For example, pipeline on the west of USA extends for more than 2500 km carrying 50 Mt CO_2 annually (IPCC.2005). However, these distances have only been possible in the oil and gas industry because of the high market value for oil and gas. In CCS there is, currently, no economic interest associated with CO_2 storage. Therefore, setting up a pipeline network is a challenge especially for distances exceeding 300 km. This is because pipeline network requires a good economic situation: regulation, classification of CO_2, health issues, liability and the cost of pipeline infrastructure development may be a challenge to some countries (CSLF, 2011).

If CO_2 is to be transported by pipeline through a densely populated area, various safety measures and CO_2 purity are required. For example, if the pipeline goes through a populated area, overpressure and leak detection will need to be installed and the concentration of H_2S (which is a colourless, very poisonous, flammable gas) will have to be very low (IPCC, 2005). Similar specifications are expected when considering the type of steel to be used to construct the pipeline.

Moreover, CO_2 needs to be dehydrated and compressed before transportation. The dehydration specifications are mostly dependent on the type of steel used for making the pipeline. For example, if the steel pipeline is made of carbon-manganese metal, CO_2 does not corrode the metal if the humidity is less than 60% (IPCC, 2005). CO_2 is subsequently cooled and compressed to about 150 times the atmospheric pressure for cost and transport efficiency (CSLF, 2011).

Other possible means of transporting CO_2 include truck/road, rail and ship. Road and rail transportation are generally use to transport CO_2 in small quantities i.e. for use in the food and beverage industry, but are not favoured for transporting large quantities of CO_2. This is because of possible accidents that might result in asphyxiation, additional CO_2 emission and energy inefficiency. On the other hand, ships are used for this operation since they are mostly isolated from the public. Large scale ship transportations of CO_2 are already in existence, particularly in the oil and gas industry (IPCC, 2005).

2.1.3 Storage

The final stage of CCS is the storage of CO_2 into geological formations, in ocean floor, in the form of mineral carbonates or for use in industrial processes. Storing CO_2 in geological

formations and in the ocean always require some form of monitoring and verification during and after injection. For the purpose of this study the focus will be on geological storage and mineral carbonation. Each of these storage options will be discussed in more details in the sections below.

2.1.3.1 Geological Formation

The three most commonly used forms of geological storage are depleted oil/gas reservoirs, saline formation and unminable coal seams. The latter is the most evasive of the three because such seams are commonly defined in terms of availability of technology and economic status. Both factors are well known to evolve with time. Therefore, if a decision is made to store CO_2 in a coal seam that is considered unmineable, the possibility of mining it at a later stage should be ruled-out permanently. Even if the technology becomes available, and the economy is in a good state, because mining such seams will result into a release CO_2 back to the atmosphere. Some details were omitted on unmineable coal seams because this study is mostly focusing on saline formation and depleted oil/gas reservoirs.

To date, more than 16 CCS projects are conducted successfully world wide on different scales. From these, four are still underway on commercial scale namely Alberta Basin project in Alberta & B.C., Canada; Snøhvit project in Barents Sea, Norway; Sleipner project in North Sea, Norway and In Salah project in Krechba, Algeria (Michael, 2010). The highest injection rate for a single storage operation is currently about 1 Mt CO_2/year and about 20 Mt of CO_2 was successfully injected into saline reservoirs by the end of 2008 (Michael, 2010). This is, however, still very low when compared to the annual global CO_2 emissions.

Saline reservoirs provide the largest CO_2 storage capacity globally, which is estimated to be between 400 and 10 000 Gt CO_2, followed by depleted oil and gas reservoirs at 920 Gt, and lastly unminable coal seams at 15 Gt (IEAGHG, 2005), because of poor characterization in the context of CCS. Although saline formation provides the largest storage potential, oil/gas reservoirs are the most preferred CO_2 storage sites, for the following reasons:

- Proven structural and stratigraphic trapping (demonstrated integrity and safety)
- Extensive studies and characterisation of geological and physical properties of oil and gas fields

- Computer models have been developed to predict the moment, displacement behaviour and trapping of hydrocarbons
- Infrastructure and wells already in place that can be used for CO_2 storage

In contrast, saline formations exhibit the following challenges:

- Distance from point sources: Putting pipeline infrastructure that is longer than 300 km in place may be a great challenge to countries without a strong economy.
- They do not produce any product of economic value: for instance, the enhanced oil recovery (EOR) produces oil that can generate an income that will cover the cost of CO_2 transportation.
- Its structural and stratigraphic trapping is not proven

The geological formations that are considered for CO_2 storage are characterised by depth, thickness, and with depleted hydrocarbons or containing unusable groundwater (Table 2.1). It is important to note that the properties are reservoir-dependent and may vary from country-to-country. The reservoir conditions are specified in order to optimise storage capacity and to make it as safe as possible. Below 800 m depth, CO_2 is in a supercritical state meaning "it can disperse through the pore of solids without molecules colliding, like a gas, and materials can dissolve in it, like a liquid" (ICCS, 2009). The density of sc-CO_2 increases and its volume decreases with increasing depth, as presented in Figure 2.2, thus allowing larger quantities of sc-CO_2 to be stored below 800 m. However, this may be a challenge if the reservoir has high geothermal gradient. This is because CO_2 is more soluble at lower temperature and higher pressures. Therefore, colder basins are considered more favourable for CO_2 storage than warm basins. In warm basins the capacity is reduced in terms of CO_2 mass due to higher CO_2 buoyancy, which drives the CO_2 migration upward (Bachu, 2003).

Table 2.1: Preferred reservoir characteristics for CO_2 storage (Modified from the South African CCS School conducted by TNO, SACCCS and CGS, 2011)

Parameters	**Properties**
Depth	Between 800 m and 2500 m
Types of Caprocks	Impermeable (shale, evaporates)
Caprock thickness	> 100 m
Reservoir thickness	> 50 m
Reservoir rock types	Permeable and porous (sandstone)
Reservoir Porosity	> 10%
Reservoir Permeability	> 300 mD
Salinity	> 100 g/L

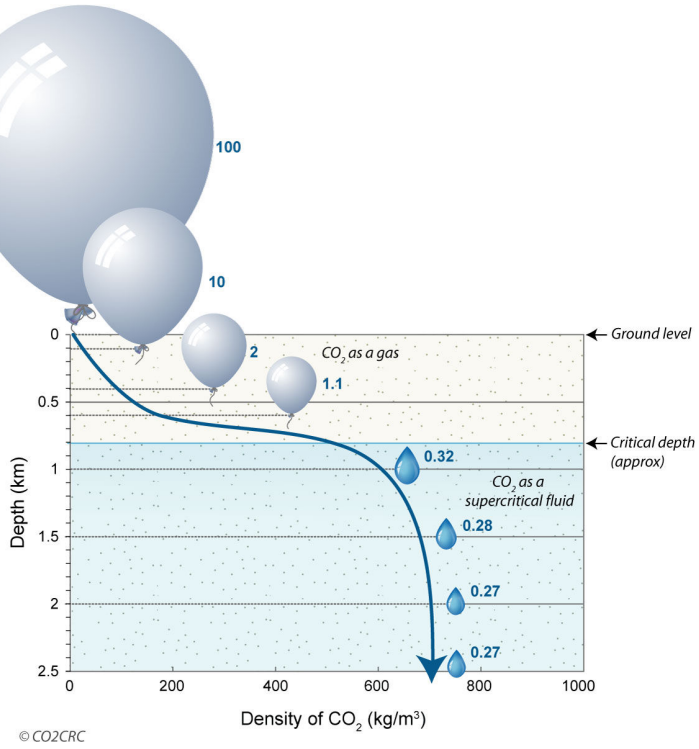

Figure 2.2: At greater depth CO_2 density increases which enables larger quantities of CO_2 to be stored in a relatively small volume (Kaldi el al., 2008)

2.1.3.2 CO_2 Trapping Mechanisms

The success of storing CO_2 in saline formations and depleted oil/gas reservoirs is largely dependent on their ability to confine CO_2 long enough to form stable carbonates, as shown in Figure 2.3. This phenomenon is referred to as trapping, and can be sub-divided into physical and geochemical trapping mechanisms, discussed in more details below.

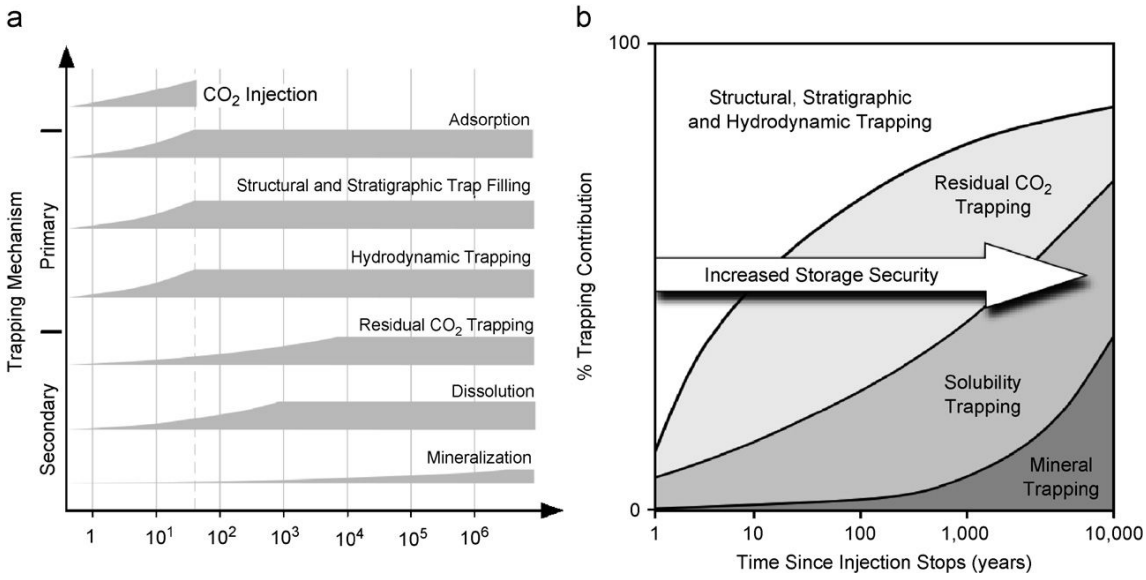

Figure 2.3: Storage security with respect to time as a result of trapping mechanisms (Bachu et al., 2007)

2.1.3.2.1 Physical Trapping Mechanisms

Physical trapping refers to an immobilization of CO_2 in its gaseous, liquid or supercritical state as a free-phase substance within a volume of a geological medium.
Physical trapping mechanism can be subdivided further into (Bachu, 2008):

- *Static trapping* of mobile CO_2, which can either be in stratigraphic and structural or even man-made caverns. Static trapping occurs below the caprock (e.g. shale, mudstone), and is a prerequisite for storing CO_2 in geological formations. Structural trapping involves folded, faulted or fractured rocks, whereas stratigraphic traps are formed by changes in rock type caused by variation in the setting in which the rocks were deposited.

- *Residual-gas trapping/hydrodynamic trapping* in the pore space at irreducible gas saturation, in which case the CO_2 is immobile (Figure 2.4) because of the interfacial tension between CO_2 and formation water as well as non-wetting gas in a water-wet porous medium (IEAGHG, 2011). Flow is not possible even if a pathway is available. This is mostly related to immiscible fluid phases (Johnson et al., 2002).

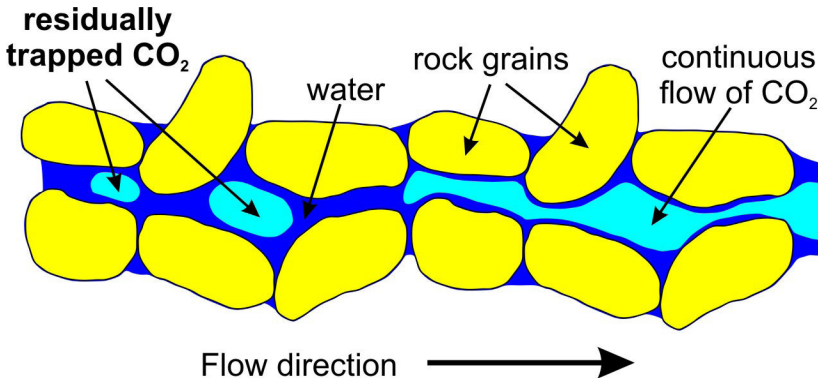

Figure 2.4: Geological reservoir showing porous rock, permeable and diffused CO_2 (Kaldi et al., 2008)

2.1.3.2.2 Geochemical Trapping

The solubility of sc-CO_2 depends on temperature, pressure, pH, and salinity. These factors are paramount when coming to geochemical trapping mechanisms. The dissolution of CO_2 in water is reduced at temperatures greater than 120°C at lower pressure (Lu et al., 2009). This factor will affect the formation of carbonate minerals if there is less CO_2 available in solution. In addition, pH will also affect the formation of carbonates because carbonate minerals form at pH greater than 8. Geochemical trapping mechanism is particularly attractive since it would in principle ensure CO_2 immobilization for very long periods of time, provided that no tectonic movements or other disturbance occurs after the injection.

The geochemical trapping CO_2 is mostly related to: direct interaction of the immiscible plume with formation water and indirect interaction between the plume and formation minerals through the aqueous wetting phase (Johnson et al., 2002). Geochemical trapping can also involve the adsorption of CO_2 onto organic materials contained in coals and shale as well as the dissolution in subsurface fluids, in which case it is referred to as solubility, see equation 2.1 (Bachu et al., 2007).

$$CO_2\,(g) + H_2O\,(\ell) \rightleftharpoons H_2CO_3\,(aq) \rightleftharpoons HCO_3^-\,(aq) + H^+ \rightleftharpoons CO_3^{2-}\,(aq) + 2H^+\,(aq) \quad (2.1)$$

The second scenario is where dissolved CO_2 reacts to form carbonic acid, which can react with sodium, potassium, calcium, iron or magnesium to form bicarbonate (equation 2.2 and 2.3).

$$3\,KAlSi_3O_8\,(s) + 2\,H_2O\,(\ell) + 2\,CO_2\,(g) \rightleftharpoons KAl_2(AlSi_3O_{10})(F,OH)_2\,(s) + 6\,SiO_2\,(s) + 2\,K^+\,(aq) + 2\,HCO_3^-\,(aq) \quad (2.2)$$

$$3\,KAlSi_3O_8\,(s) + H_2CO_3\,(aq) \rightleftharpoons KAl_2(AlSi_3O_{10})(F,OH)_2\,(s) + 6\,SiO_2\,(s) + 2\,K^+\,(aq) + 2\,HCO_3^-\,(aq) \quad (2.3)$$

Lastly, geochemical trapping can take place by means of mineral trapping (equation 2.4), where CO_2 is finally converted into thermodynamically stable carbonate minerals. This process is very slow and may take over hundreds to thousands of years (IPCC, 2005).

$$CO_3^{2-}\,(aq) + Ca^{2+}\,(aq) \rightarrow CaCO_3\,(s) \quad (2.4)$$

2.2 Underground Storage

The concept of injecting waste material underground is not new. This technology has been used in the past to inject hazardous material and acidic gas into geological formations. For example, 2.5 Mt CO_2 and 2.0 Mt H_2S have been injected into saline formations and depleted hydrocarbon reservoirs in the Alberta Basin from 1990 to 2003 (Bachu and Gunter, 2004).

The injection of CO_2 underground has further been supported by the existence of natural accumulation of CO_2 in a mixture with other fluids underground. This is a widespread phenomenon in many geological basins, especially in North America, Europe and Australia. Some of these deposits are stored in secure and impermeable traps, whereas others are unstable and leaking (Stevens et al, 2001). Most of these CO_2 storage reservoirs have similar geology to that of natural gas fields, with the gas trapped in dome-like structures. The typical reservoir lithologies consist of sandstone and dolomite, where mudstone, rock salts and anhydrite form the cap-rocks, for example, McElmo Dome, Sheep Mountain, and Bravo Dome in the southwestern U.SA (Stevens et al., 2001). South Africa does posses a similar feature along the Bongwan gas fault located in Eastern Cape (former Northern Pondoland and Alfred County) and KwaZulu Natal (Gevers, 1941).

2.3 Mineral Carbonation

Another technology forming part of the CCS portfolio is CO_2 sequestration by mineral carbonation. This concept was first proposed by Seifritz (Seifritz, 1990). Mineral carbonation mimics the naturally occurring geological process whereby CO_2 and silicate minerals react to form thermodynamically stable carbonates (equation 2.5).

This process has been recognized as a permanent and safe means of storage for anthropogenic CO_2. Moreover, it can be accurately referred to as sequestration whereas the other forms of "sequestration techniques" represent storage (Kaszuba et al., 2005). This process is, however, very slow, energy-demanding and expensive (Teir, 2008). In order for this process to be adopted on an industrial scale, the kinetics of the mineral carbonation reaction will need to be improved (within hours) in an economic manner.

$$(Mg,Ca)_xSi_yO_{(x+2y)}\ (s) + x\ CO_2\ (g) \rightarrow\ x\ (Mg,Ca)CO_3\ (s) + y\ SiO_2\ (s) + heat \qquad (2.5)$$

This technology is strongly considered as an alternative to geological sequestration by countries such as Finland and Korea where geological storage is not possible (Sipila et al., 2008). This is because the geology in these countries is characterized by metamorphic rocks, as it is largely the case in South Africa. The state of the art of the technology has been recently reviewed by several authors like Doucet (2011) and Torrontegui (2010). This process can be approached by using either direct or indirect mineral carbonation, which are discussed below.

2.3.1 Direct Mineral Carbonation

Direct mineral carbonation is the simplest and a single step approach to mineral sequestration. It can be conducted in two ways: direct dry gas-solid reaction or via an aqueous solution.

2.3.1.1 Direct Gas-Solid Carbonation with CO_2

As the name suggests, this is the process where gaseous CO_2 is reacted directly with a solid material (equation 2.6) e.g. olivine or Ca/Mg rich solid. The major advantage of direct gas-

solid carbonation is that the heat generated during the carbonation process can be applied further, a process which is still under investigation (Huijgen and Comans, 2004). However, high CO_2 pressures are required for reasonable reaction rates.

$$Mg_2SiO_4\,(s) + 2\,CO_2\,(g) \rightarrow 2\,MgCO_3\,(s) + SiO_2\,(s) \quad (2.6)$$

Whilst most research groups have abandoned this route, this process is still actively researched by Prof Zevenhoven's group in Finland (Doucet, 2011). The investigated process involves reacting Mg-rich silicates with ammonium sulphate salt in a solid-solid reaction (Nduagu and Zevenhoven 2010). In this process magnesium sulphate is produced by reacting magnesium silicate and ammonium sulphate at temperatures between 400-500°C (equation 2.7). Magnesium sulphate is then dissolved in water and treated with ammonium hydroxide to form magnesium hydroxide (equation 2.8). After crystallisation, solid magnesium hydroxide is reacted with gaseous CO_2 in a fluidised bed reactor to form magnesium carbonate (equation 2.9).

$$Mg_2SiO_4\,(s) + 2\,(NH_4)_2SO_4\,(s) \rightarrow 2\,MgSO_4\,(s) + 4\,NH_3 + SiO_2 + 2\,H_2O\,(g) \quad (2.7)$$

$$MgSO_4\,(s) + 2\,NH_4OH\,(aq) \rightarrow Mg(OH)_2\,(s) + (NH_4)_2SO_4\,(aq) \quad (2.8)$$

$$Mg(OH)_2\,(s) + CO_2\,(g) \rightarrow MgCO_3\,(s) + H_2O\,(\ell) \quad (2.9)$$

2.3.1.2 Aqueous Scheme

The aqueous scheme concept is based on the fact that water can significantly enhance the reaction rate in natural rock weathering (equation 2.10). This route was developed by the Albany Research Center (ARC) on the basis of forming carbonic acid. The solid silicate mineral is carbonated directly in water at elevated CO_2 pressure and temperature (Huijgen and Comans, 2004):

$$Mg_2SiO_4\,(s) + CO_2\,(g) + 2\,H_2O\,(\ell) \rightarrow 2\,MgCO_3\,(s) + H_4SiO_4\,(aq) \quad (2.10)$$

2.3.2 Indirect Mineral Carbonation

In this process the reactive components i.e. Ca and Mg are firstly extracted from the feedstock in solution before being reacted with CO_2. Thereafter, the reactive components can carbonate relatively easily in a separate step.

The first step in indirect mineral carbonation is where a strong (e.g. HCl, HNO_3), weak (e.g. NH_4 salts) or organic (e.g. acetic acid) acid is used to extract the reactive components. The feed stock can be treated even further, depending on the purpose (e.g. cases where the feedstock contains valuable metals or minerals that could be extracted before carbonation) after which it can be carbonated. For example, a plagioclase feedstock can be treated with NaOH to enhance the extraction of calcium from its 3-dimensional structure in which it is kept by silicon and aluminum (Blencoe et al., 2004) and/or for "pH swing" i.e. to increase the pH to favour carbonation.

2.3.3 Sources of Ca and Mg for mineral carbonation

Various materials have been proposed (Figure 2.5), as the source of alkaline ions that can possibly be carbonated. Carbonation of the Ca- and/or Mg-rich primary minerals (e.g. olivine, serpentine, and wollastonite) is possible but it is not currently economically-viable (Doucet, 2008).

As an alternative to primary minerals, alkaline wastes have been proposed. Alkaline waste materials are much more reactive than primary minerals, but are available in smaller quantities. Waste materials are more favourable than primary minerals because they have a higher carbonation rate, high reactivity, are available at low cost, and may have a high Ca, Mg and Fe content.

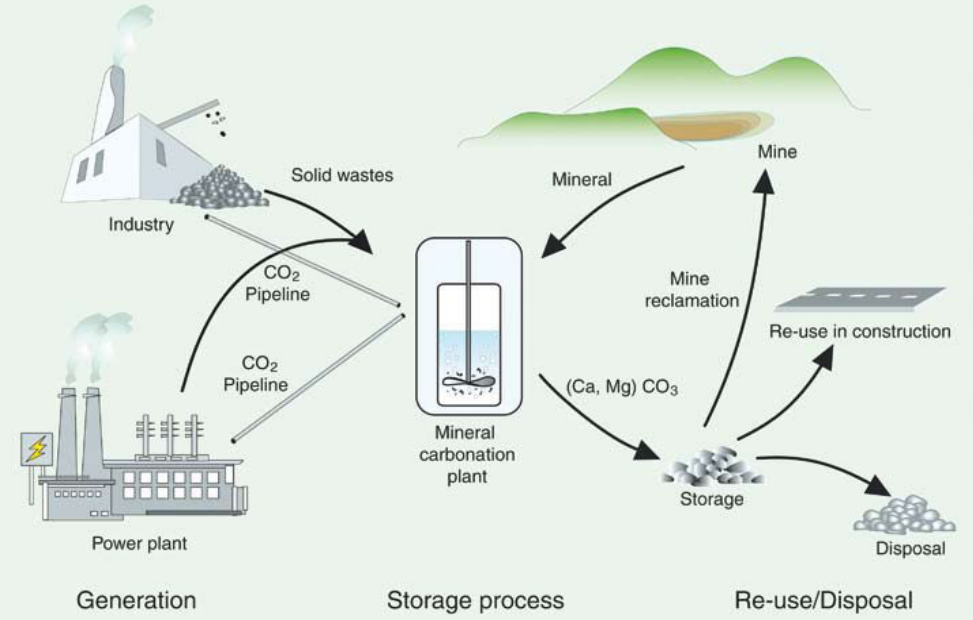

Figure 2.5: Schematic representation of an industrial mineral carbonation flow sheet (IPCC, 2005)

2.4 Integrity of the reservoir

The key to the development of geological sequestration in saline formation is the existence of suitable, high-integrity geological sites for safe, long-term CO_2 storage. However, it is virtually impossible to predict the reservoir integrity with 100% certainty. Nevertheless, it is very important to at least identify all contingencies and possible remediation scenarios prior to CO_2 injection. Such as the sudden release of natural CO_2 as a result of tectonic activity, like in Lake Monoun and Lake Nyos, in Cameroon, that resulted in 1700 and 37 fatalities, respectively (IEAGHG, 2006). Therefore, areas that show a possibility of a tectonic event will have to be avoided.

Other contingencies as identified by NETL (2008) include:

- Pressure caused by CO_2 injection could result in migration of fluids into nearby freshwater aquifers and natural resources
- The increase in pressure in the reservoir could cause structural deformation that will create an escape route
- CO_2/brine mixture could react with cement plugging the wells, thus creating escape route or improve sealing

Price and Oldenburg (2009) also presented a brief discussion on the possible consequences of failure to the storage site:

- If CO_2 leaks into an aquifer; water will acidify and produce carbonic acid. The acidic water could dissolve minerals thereby releasing naturally occurring elements such as arsenic, lead, or other heavy metals that can contaminate the water.
- If CO_2 leaks to the surface or the near subsurface, plants (particularly if the soil pH is varied) and O_2-breathing life could be harmed.

The CO_2 dissolution in brine or water results in the formation of carbonic acid, which results in the reduction of pH. Acidic conditions could result in the alteration of the rock cavities (Schaef and McGrail, 2005). This may either cause the dissolution of primary minerals, secondary minerals and/or the precipitation of secondary minerals.

Precipitation of secondary minerals may cause in turn increased alkalinity. Some of the possible reactions are presented below (Pirajino, 1992)

In equation 2.11, H^+ ions are consumed from the solution which becomes more basic until the K-feldspar is used up. The new mineral assemblage is muscovite and quartz.

$$^1/_2\,KAlSi_3O_8\,(s) + H^+\,(aq) \rightleftharpoons {}^1/_2\,KAl_3Si_3O_{10}(OH)_2\,(s) + 3\,SiO_2\,(s) + K^+\,(aq) \qquad (2.11)$$

A continuing reaction (equation 2.12) upon the products of the above K-feldspar hydrolysis will produce kaolinite:

$$KAl_3Si_3O_{10}(OH)_2\,(s) + H^+\,(aq) + 1.5\,H_2O\,(\ell) \rightleftharpoons 1.5\,Al_2Si_2O_5(OH)_4\,(s) + K^+\,(aq) \qquad (2.12)$$

In the presence of plagioclase in the same rock, simultaneously pyrophyllite will be formed (equation 2.13):

$$2\,NaAlSi_3O_8\,(s) + 2\,H^+\,(aq) \rightleftharpoons Al_2Si_3O_{10}(OH)_2\,(s) + 2\,SiO_2\,(s) + Na^+\,(aq) \qquad (2.13)$$

In the above reactions, further H^+ ions are used up and the fluid becomes more basic and K and Na- rich. The above reactions thus inevitably result in consumption of H^+ and formation of a progressively more alkaline fluid.

The reaction of a simple mineral assemblage with water can thus result in a multi-component reaction with new mineral assemblage, even if the system remains isochemical. The alteration products will be more complex in an open chemical system, in which the dissolved chemical components in the fluid, other than H^+, also take part in the reactions.

The accumulation of base cations in the fluid by H^+ consumption will effect the alteration downstream of the fluid flow direction, where the base cations can react with the wall rock ("cation metasomatism") e.g. (equation 2.14 and 2.15):

$$2\ NaAlSi_3O_8 + 4\ (Mg,Fe)^{2+} + 2\ (Fe,Al)^{3+} + 10\ H_2O \rightarrow (Mg,Fe)_4(Fe,Al)_2Si_2O_{10}(OH)_8 + 4\ SiO_2 + 2\ Na^+ + 12\ H^+ \quad (2.14)$$

or

$$3\ CaMg(CO_3)_2 + 4\ SiO_2 + 6\ H^+ + 4\ H_2O \rightarrow Mg_3Si_4O_{10}(OH)_2 + 6\ H_2CO_3 + 3\ Ca^{2+} \quad (2.15)$$

By addition of e.g. Fe, Mg and Al from the fluid, plagioclase will be chloritised and a significant amount of H^+ will be produced. Consequently the acidity of the fluid will be increased. Any fluid in the same rock can thus become more basic on its pathway, and subsequently more acidic, when reacting with the same or with another rock, and produce different mineral assemblages.

The above reactions of course still leave factors like lithostatic and hydrostatic pressure, compaction at changing pore volume and permeability, fluid/rock adhesion, pore-neck morphology and blockage etc. untouched. Nevertheless, these are equally important in reservoir evaluation. The aforementioned activities are a possibility but they can be prevented by thorough characterisation of the reservoir prior to injection.

The ranges of reactions taking place in the subsurface upon injection of CO_2 are fairly complex and are reservoir-dependent. At one geological site, these reactions may yield an increased storage capacity within the target horizon, or may lead to increased potential for leakage beyond the confining layers. On the other hand, the displacement front formed by the sc-CO_2/brine mixture could also entrain and deposit fine particles (clays, sands) which in turn could obstruct the flow. The same effect can result from fast reaction of the injected fluid with formation minerals and precipitation of carbonates around the injection site. This would be accompanied by a decrease in permeability or reduced injectivity.

The injection of CO_2 into deep saline formations causes acidification of the brine water, which in turn impacts on the geochemical dynamics of the system. The work conducted at the Albany Research Centre (ARC), USA, has demonstrated the alteration of rock cavities due to the injection of CO_2 in a brine solution (O'Connor and Rush, 2005). This experiment was conducted using the Mt. Simon sandstone core at 35°C and 96.53 bar for 1.5 hours. The alteration of rock cavities was observed in the form of a measurable increase in porosity and similar changes in permeability, due to the aggressive properties of the sc-CO_2/brine mixtures. The porosity increase was between 4.7 and 13 % whereas permeability changes were between -10.1 and 2.0 %

Lu et al. (2010) also observed the dissolution of feldspars and conversion of smectite to form illite, allophane and carbonate minerals of a Navajo Sandstone, at 200 °C and 300 bar. These reactions are likely to increase the bulk porosity of the sandstone, but the formed illite and allophane can possibly fill the pores in sandstone grain (Lu et al., 2010). There is a considerable volume increase when clay minerals form from feldspars. This will certainly block the sandstone pores.

2.5 Geology of CO_2 Storage Sites in South Africa

As identified by Cloete (2010), the main CO_2 storage potential in South Africa is provided by the Mesozoic sedimentary basins: Outeniqua, Orange and Durban/Zululand basins. These basins are overlain by a continental margin that comprises of 165 000 km^2 of continental shelf, down to 200 m isobath, and 400 000 km^2, out to 2000 m isobath. This continental margin around South Africa was formed as a result of the break-up and separation of the Gondwana supercontinent (shown in Figure 2.6) which started in early Cretaceous. The geology of the potential storage sites is summarised in Table 2.2.

2.5.1 Outeniqua Basin

The Outeniqua basin lies at the southern tip of South Africa, extending from the regions near Cape Town, Mossel Bay and Port Elizabeth. It is bounded by the Columbine-Agulhas Arch to the west, Port Alfred Arch to the east and Diaz Marginal Ridge to the south. This basin consists of three rift sub-basins which are separated by fault-bounded basement arches

comprised of meta-sediments of the Cape Supergroup (Broad et al, 2006). It consists of three sub-basins: the Bredasdorp, Pletmos, Gamtoos and Algoa sub-basins.

Due to the exploration of oil and gas the geology of the Bredasdorp sub-basin is well known. It covers an area of about 18 000 km^2, is 200 km long, 80 km wide, is south-easterly trending and it rarely out crops onshore, whereas, the Gamtoos and Algoa sub-basins are extensive both onshore and offshore (Broad et al., 2006).

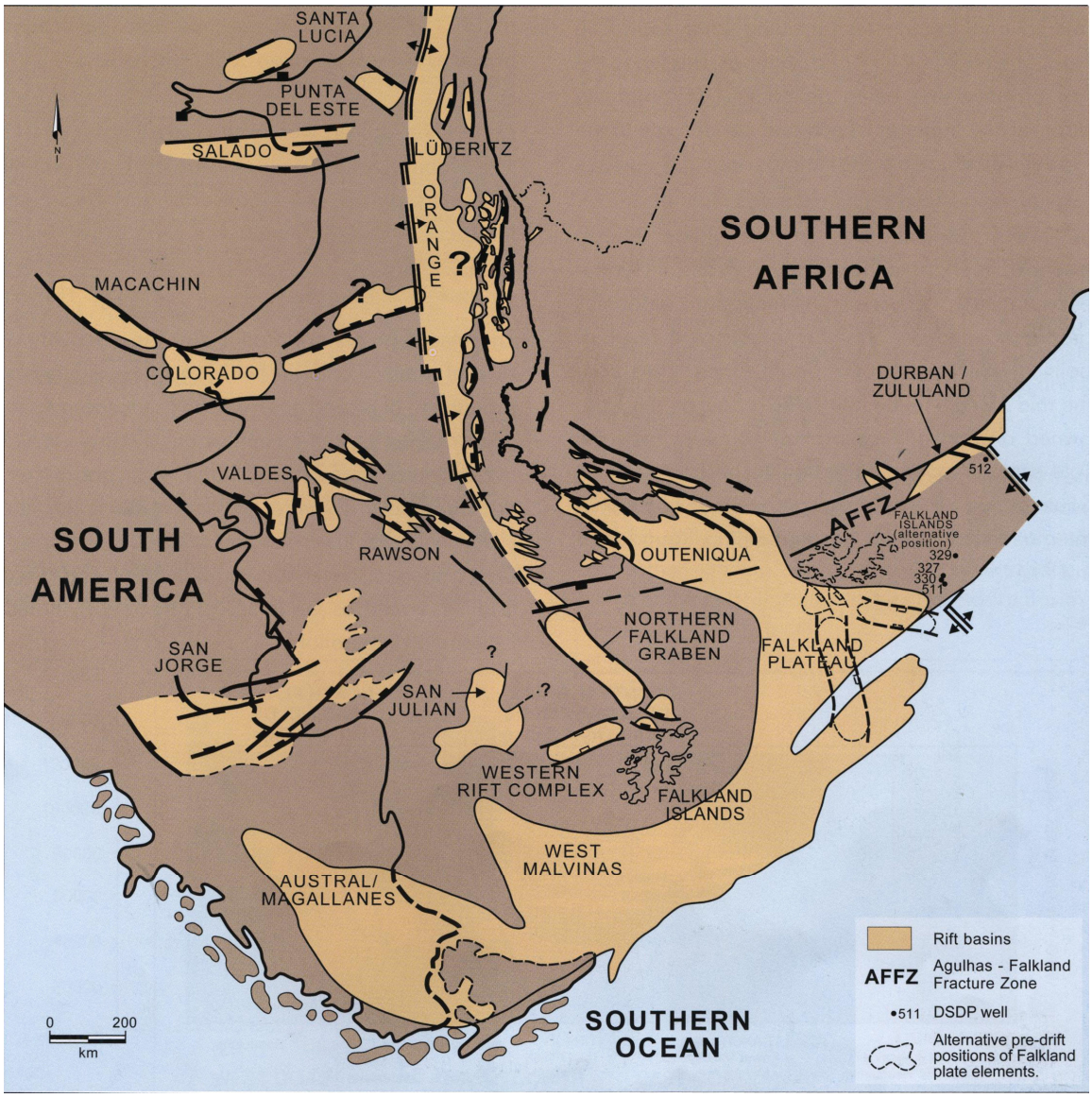

Figure 2.6: Layout of tectonic setting around South Africa in the Late Jurassic to Early Cretaceous (Broad et al., 2006)

Table 2.2: Summary of geology of the potential storage sites from Broad et al., (2006)

Basin	Sub-basin	Thickness	Lithology
Outeniqua	Bredasdorp	Up to 8000 m	Claystone, sandstone (porous and permeable), conglomerate, Glauconitic fossiliferous sandstone,
			massive glauconitic fossiliferous sandstone, organic-rich hydrocarbon shale, (floodplain and meandering deposits beach deposits)
	Pletmos	Up to 11 000 m	Lithostratigraphy is similar to that of Bredasdorp.
	Gamtoos and Algoa	~4600 m	Conglomerate, sandstone, brackish shale, marine shale, siltstone, claystone, organic-rich hydrocarbon shale
Orange		>4300 m	Volcaniclastics, organic-rich hydrocarbon shale, basaltic lava
Durban/ Zululand		~5000 m	Dolerite sill, organic-rich shale, volcanics, basalts, rhyolite, coarse grained clastic, reworked volcanics; shallow-marine, deltaic, lagoonal, glauconitic siltstone, sandstone, limestone

CHAPTER THREE
THEORETICAL BASIS FOR IMPROVING THE INTEGRITY OF SALINE FORMATIONS FOR CO_2 GEOLOGICAL STORAGE

3.1. Introduction

According to EAR (2010), the South African power generator, Eskom, produced 36.01 million tonnes of coal-combustion fly ash in 2010. About 5.6% was reused for the production of cement. The remaining 33.89 million tonnes were safely disposed and managed on Eskom ash dumps and dams, which are located adjacent to their corresponding power stations. South Africa has a long history regarding the development of new applications for this material. For instance, Ash Resources, South Africa's leading manufacturer and supplier of fly ash products, has pioneered the re-use of fly ash and has positioned itself as one of the world leaders in ash technology over the last 30 years. South Africa remains very active in the development of ash technologies (Kruger, 2003).

Fly ash is defined by Kruger (2003) as a fine powdery material composed mainly of non-combustible inorganic material containing some carbon left over from incomplete combustion. Fly ash can be classified into cementitious i.e. Class C: $SiO_2 + Al_2O_3 + Fe_2O_3$ min 50% and pozzolanic i.e. Class F: $SiO_2 + Al_2O_3 + Fe_2O_3$ min 70% (Kruger, 2010).

The typical South African fly ash is composed of amorphous phase, mullite, quartz, anhydrite, magnetite and haematite. However, the actual composition of fly ash may differ depending on the composition of the coal, the comminution technique used to prepare the pulverized fuel, the type of burner, combustion conditions and the ash recovery system itself (Kruger, 1997).

In South Africa, research and development (R&D) involving fly ash includes recovery of alumina, soil amelioration, waste immobilization, refractories, clay bricks, road stabilization, processing aids and fillers for polymers, zeolites, counteracting acid mine drainage, mine backfilling, functional fillers for rubbers as well as usage as cement extender (Kruger, 2005).

In 2006, Soong proposed the use of fly ash and brine for CO_2 sequestration. Since then research involving the usage of fly ash in carbon sequestration has received enormous attention. This is exemplified by the number of scientists, through out the world, working on the carbonation of fly ash, and at least two pilot plants exist to date: in USA and Germany. Thus far, all the work undertaken in these institutions is conducted under subcritical CO_2 conditions i.e. below 73.8 bar and 30.98 ˚C.

This study seeks to introduce a relatively new research branch involving fly ash; the injection of fly ash in a form of slurry at strategic sites of deep saline formations. The purpose of this injection strategy is to prevent the migration of injected anthropogenic CO_2 plumes beyond the confining layers of the formations, via induced in *situ* localized, accelerated mineral carbonation.

3.2 Conceptual Strategy for Fly Ash Slurry Injection and Carbonation for Improved Geological Reservoir Integrity

The most widely advocated method of CCS involves the injection of CO_2 in dense, supercritical liquid form into pore spaces in underground geological formations (see Figure 3.1). Saline formations located at depths greater than 800 m are of particular interest for countries which do not possess large depleted gas and oil reservoirs, such as South Africa (Cloete, 2010). It is, however, widely acknowledged that South Africa unfortunately lacks natural world-class storage reservoirs, although some onshore and/or offshore basins may offer storage opportunities (Cloete et al., 2007).

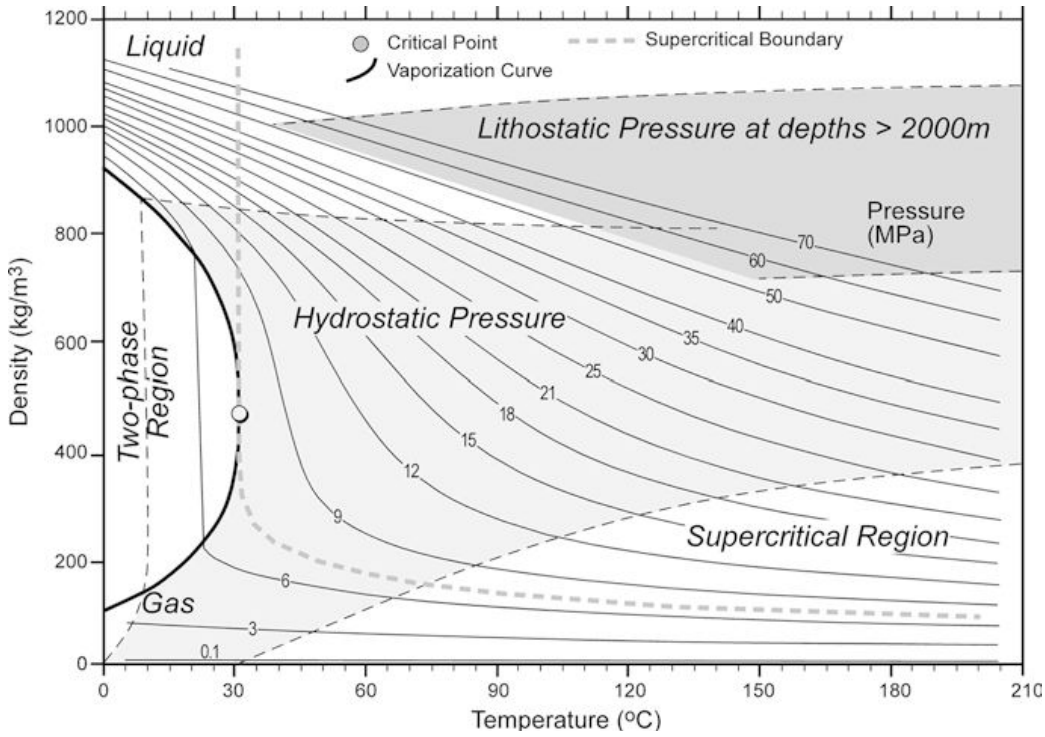

Figure 3.1: Illustration CO_2 density variation as a function of temperature and pressure (Bachu, 2003)

The Albany Research Centre (ARC) has partially demonstrated the usage of ultramafic mineral slurries (e.g. olivine, serpentine as a reactive matrix for accelerated carbonation) and CO_2 to be feasible at typical saline reservoir conditions found below 800 m depth. This involves the co-injection of mineral slurry along with CO_2 into a geological formation, to induce a localized carbonate concretion, in other to improve the reservoir integrity.

This concept would be applicable to the cases where an increase in the potential for leakage due to increased porosity and permeability of the formation or in the cases where a saline formation is perfectly suitable for CO_2 sequestration, except for the presence of a small number of minor fractures. In the South African context, coal-combustion fly ash is thought to be suitable for this application, because fly ash is abundant, readily-available at low-cost and generally much more reactive than primary mineral deposits. It could therefore provide calcium (Ca) and magnesium (Mg) ions to accelerate the precipitation of CO_2 as mineral carbonates, it has good rheology and it can be classified into very small grain sizes (sub-45µm).

Although other alkaline wastes such as steel furnace slags could also be used as sources of Ca and Mg for mineral carbonation, they are generated in much smaller amounts than fly ash. They also would require milling down to sub-45 µm size range (and most probably even lower) to minimize the risk of clogging the pores of the saline formation, which would inhibit the possibility for further injection of the slurry.

The in *situ* mineral dissolution and precipitation processes, under the influence of sc-CO_2, may have a strong bearing on the permeability and reservoir and sealing capacity of the given formation. The proposed application falls within the CCS initiative by geological sequestration and aims at improving the integrity of deep saline formations which may be at risk of leakage upon injection of CO_2. This will prevent unwanted CO_2 migration outside the boundary layers of the reservoir. Moreover, if an increase of porosity and permeability occurs, due to the aggressive properties of sc-CO_2/brine mixtures or where the presence of minor fractures in the saline formation cannot be excluded.

Understanding the reactivity of the storage reservoir rock (e.g. sandstone) of the saline formations with injected CO_2 is essential to predict the short-, medium- and long-term fate of CO_2. Whilst significant effort has been made to better comprehend CO_2 mineralization via carbonate precipitation (Lu et al., 2010), a lesser amount of information is available on CO_2/brine/rock interactions following CO_2 injection. It is however known, that depending on the nature of the CO_2/brine/rock interactions may either:

- increased porosity and permeability (O'Connor, 2005), which may result in greater storage capacity of the intended reservoir or unwanted CO_2 migration outside the boundary layers of the reservoir
- or decreased porosity and permeability with reduced injectivity due to carbonate precipitation (Lu et al., 2010)

Another aspect to be taken into account, is that the feasibility of sequestration of CO_2 by aqueous carbonation of coal-combustion fly ash and steel furnace slags has already been demonstrated under sub-critical CO_2 conditions (e.g. Huijgen and Comans, 2006; Montes-Hernandez et al., 2009). This has not been demonstrated with brine waters under supercritical CO_2 conditions, such as those found at geological depths greater than 800 m. This work is demonstrating the extent and rate of conversion of sc-CO_2 when reacted with coal-

combustion fly ash in synthetic brines and at different T/P conditions, which infer various densities, hence reactivity, to sc-CO_2.

3.3 Methodology

The hypotheses mentioned in Chapter 1, were approached as three separate work packages (WP).

WP1: Carbonation of synthetic brine where NaOH is used to increase the pH above 8 under supercritical CO_2 conditions

This WP involves the carbonation of synthetic saline brine under sc-CO_2 conditions, where NaOH is added to increase the pH above 8. Several conditions are selected such that the temperature is above 31 °C and the pressure is above 73 bar. The reactions will be conducted using a Parr high temperature-pressure reactor (section 4.5). The liquid samples will be analysed using ICP-MS and the solids will be analysed using XRD (mineralogical composition) and SEM (morphology and crystal types of formed carbonate products).

WP2: Carbonate precipitation in CO_2-fly ash systems under supercritical CO_2 conditions

The feasibility of mineral sequestration of CO_2 by aqueous carbonation of fly ash has already been demonstrated under sub-critical CO_2 conditions, but not under sc-CO_2 conditions such as those found at depths greater than 800 m. This WP aims at demonstrating the extent and rate of conversion of sc-CO_2 when reacted with calcium and magnesium from fly ash. The Pressure (P) and Temperature (T) must be greater than 73 bar and 31 ºC, respectively, in order for CO_2 to be in the supercritical state. Different T/P combinations infer various densities of CO_2, hence reactivity might vary. For the purpose of this WP, fly ash was selected and reacted with industrial-grade sc-CO_2 of distinct densities under varying T/P conditions (see Chapter 4). Reactions took place in a high-pressure, high-temperature reactor which is supplied by a CO_2 line (see Chapter 4).

Variables to be tested include T/P, partial pressure of CO_2, S:L ratio and reaction time. Untreated fly ash and fly ash treated with sc-CO_2 for varying periods and under different experimental conditions were then characterized by several techniques, including XRD

(mineralogical composition), XRF (elemental composition), SEM (morphology and crystal types of formed carbonated products). The amount of CO_2 converted to carbonates was quantified using carbon and sulphur (C&S) analyser. The use of these complementary techniques provided a better understanding of the kinetic and mechanistic aspects of the reactions. It also helped to ascertain optimal variables to be used for optimal carbonation extent and rate to be achieved.

WP3: Simulated in-situ carbonation tests

Due to financial and time constrains this WP was not fully demonstrated. WP3 was designed to investigate the effects of sc-CO_2/brine mixtures on the porosity and permeability of sandstone cores under pressures representative of depths of 800-2000 m in the presence and absence of fly ash. Split cores of sandstone from South African saline reservoirs were supplied by the PASA. Their porosity and permeability, provided by PASA, served as a baseline for the core samples prior to the CO_2 flood tests. Their bulk mineralogical compositions were analyzed using XRD, and optical microscopic observations of their pores were performed. Brine solutions were formulated to simulate those reported within the relevant geological basins, in order to mimic the natural system as closely as possible.

These tests were supposed to be conducted at ambient pressure, representative of specific depths, and at higher pressure to simulate the expected CO_2 injection pressure. Brine solution was to be re-circulated through the core holder by placing two high-pressure autoclaves in line (upstream and downstream) with the core holder. Flood tests were to be carried out with CO_2-brine streams with or without fly ash. Tests were to be carried out over varying periods of time ranging between 500 and 4000 hours under static conditions, except for a brief stirring period once a day to simulate CO_2 injection. At completion, the cores were to be re-analyzed using the aforementioned characterization tools for comparison. Effects of CO_2/brine mixtures with and without fly ash were to be quantified. Carbonate formation could be determined using XRD and TGA-FTIR. Findings were to be discussed in the context of relevance for geological saline reservoirs.

3.4 CO_2 and mineral slurry co-injection scenarios

Three distinct scenarios for the co-injection of CO_2 and mineral slurries were proposed by O'Connor and Rush (2005) and are presented along with the personal views of the present author. This is done in order to access the feasibility of the concept of improving geological storage integrity through mineral carbonation.

3.4.1 Co-injection of the mineral slurry and CO_2 in the main injection well

It was suggested that the simultaneous co-injection of CO_2 and the mineral slurry through a single primary well may help envelope the CO_2 plume with an "engineered carbonate curtain" or barrier and thereof prevent the uncontrolled diffusion of CO_2 outside the confined layers of the saline formation (O'Connor and Rush, 2005). However, it is anticipated that this scenario would cause premature clogging of the pore spaces with newly-formed mineral carbonates at proximity of the injection well and would subsequently, and possibly rapidly, prevent further CO_2 injection. Though the usage of one well for the injection of CO_2 and the slurry has the advantage of costs reduction.

This scenario could also be achieved by injecting below the fault so that the slurry can rise along the fault and block it through mineralisation. Afterwards a sequestration borehole can be drilled as shown in Figure 3.2.

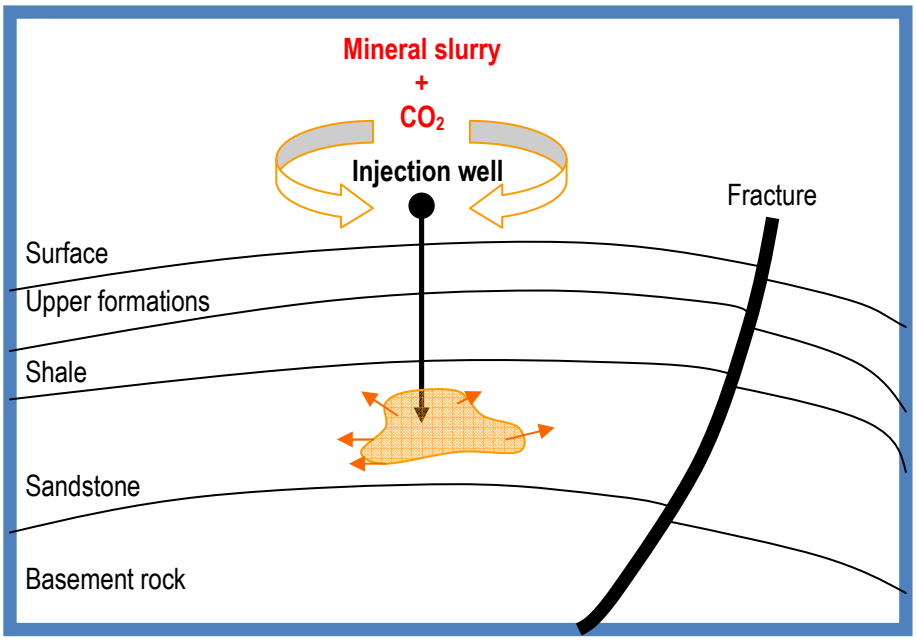

Figure 3.2: Illustration of simultaneous co-injection of CO_2 and the mineral slurry through a single well

3.4.2 Use of additional wells for injection of mineral slurry and CO_2

This scenario involves the injection of CO_2 at the primary well and that of the mineral slurry at secondary wells. This is done in order to place a mineral slurry wall at strategic places around the CO_2 plume in existing fractures or between CO_2 and fault zones or facies changes. That will promote accelerated carbonation at key areas and thereby prevent the migration of CO_2 outside the confined layers of the reservoir. Whilst this will prevent premature carbonate precipitation at the primary injection well, it will require additional costs for the drilling of secondary injection wells. Key to this scenario for horizontal isolation of the CO_2 plume will be the selection of the appropriate locations and depths of the wells with regard to zones of faults or fractures within the target formation. The appropriate well spacing, and the appropriate concentration of mineral reactant to inject into these secondary wells will also be crucial. This procedure will however, also require an extremely detailed knowledge of the lateral and vertical distribution of mineralogy and porosity of the storage horizons and the sites of possible zones of weakness of the geological seals.

The CO_2 could migrate and at the contact with the slurry will progressively convert into a "carbonated mineral slurry curtain". The "carbonate curtain" will form from the volume expansion occurring upon carbonate formation, which would fill the pore spaces between the formation grains (Figure 3.3). This will act as a barrier preventing the injected CO_2 to migrate further towards the aforementioned zone of weakness.

The secondary well could also be used to monitor the reservoir. This could potentially eliminate the cost factor since the monitoring well is required.

Scenario a) in Figure 3.3: a possible injection scenario is to have a secondary well, where the fracture is filled with mineral slurry to inhibit the excessive porosity and permeability. CO_2 will then, react with the slurry at contact to form a carbonated curtain. However, the kinetic of formation of the curtain is uncertain and the resistance of the filling to the increased pressure is also unclear.

Scenario b) in Figure 3.3: the most theoretically conceivable induced mineral carbonation in a geological formation for CO_2 sequestration is the possibility of forming a "carbonate curtain" between the zone of weakness (i.e. fault zones, fractures, facies changes) and the injection well. Key to this is the selection of the appropriate locations and depths of the wells with regard to zones of faults or fractures within the target formation, the appropriate well spacing, the appropriate concentration of mineral reactant to inject in these secondary wells and correct timing.

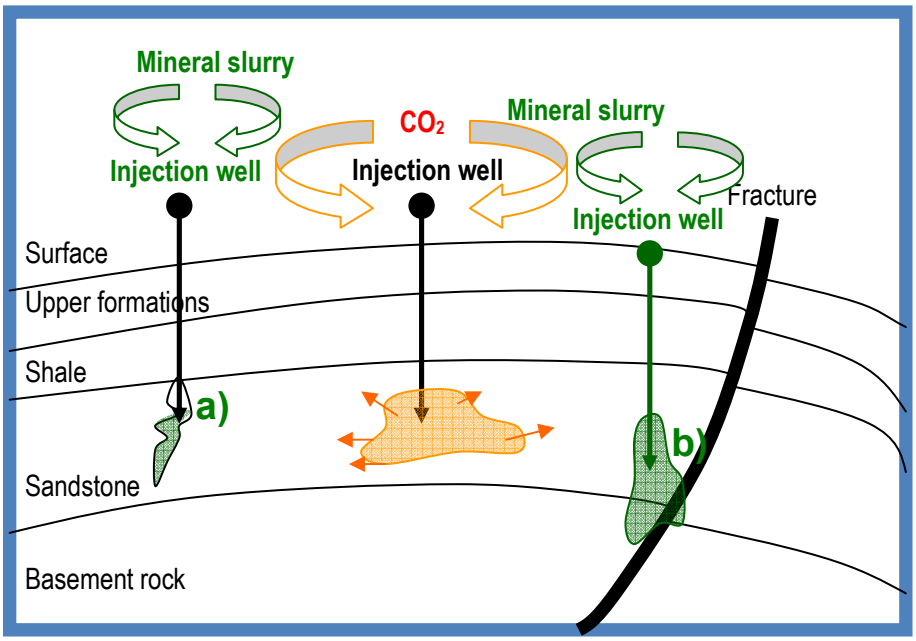

Figure 3.3: a) Fracture-filling to inhibit excessive porosity/permeability.
b) Emplacement of a slurry wall or curtain between the CO_2 flood and known fault zones or facies changes

3.4.3 Fracture-filling in the overlaying caprock

It was also proposed that minor faults in overlaying caprocks could also be filled with mineral slurries in order to ensure vertical isolation of the CO_2 plume through minimization or prevention of the risk of leakage through caprock see Figure 3.4 (O'Connor and Rush, 2005). While this approach is theoretically conceivable, it is unlikely that injection under these conditions would be well-received owing to the obvious risk of leakage which may be caused by excess pressure resulting from injection into the caprock.

A key aspect of all CCS options is the sealing efficiency of caprocks above potential CO_2 storage reservoirs. A real, continuous and ubiquitous vertical CO_2 migration process in the form of diffusive loss of CO_2 through pore spaces of the caprock (e.g. Busch et al., 2008) or by upward capillary percolation due to the re-activation of micro-fractures in the caprock (e.g. Angeli et al., 2009), is generally accepted. However, the rapid leaching by seal-breaching would represent a real, unacceptable threat in the case of fracture-filled overlaying caprocks (shale). It would also be impossible to monitor such leakage over long periods,

which is necessary as leakage sites would tend to grow through dissolution of minerals affected by acidic waters and CO_2.

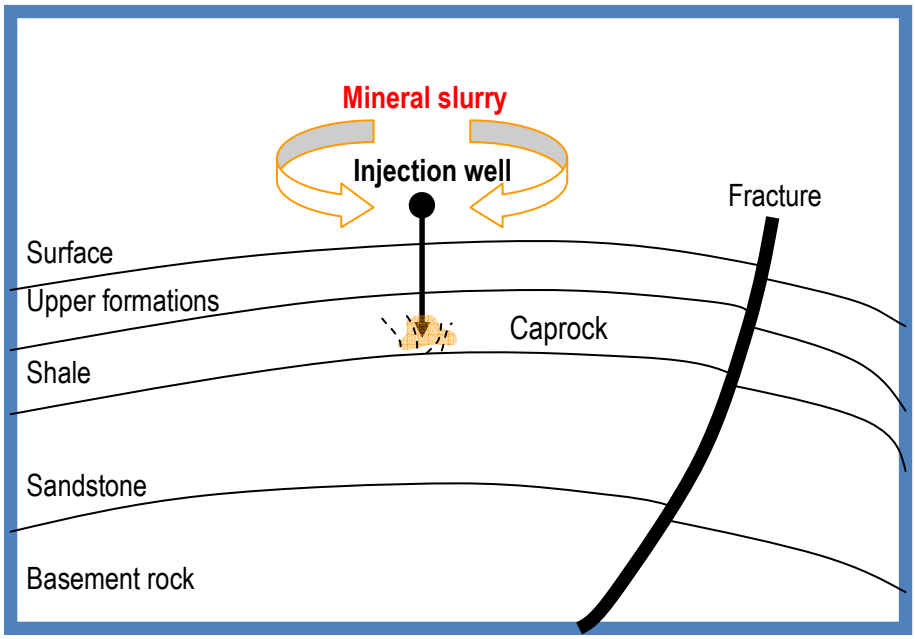

Figure 3.4: A scenario where a fault could be filled with mineral slurries in order to ensure vertical isolation of the CO_2 plume by minimizing the risk of leakage through the caprock

CHAPTER FOUR

SAMPLES AND EXPERIMENTS

4.1 Sampling of fly ash

Eight fly ash samples (Table 4.1) from South African power stations were provided by Ash Resources Pty Ltd: four samples originated from the Lethabo Power Station, three samples from the Matla Power Station and one from the Matimba Power Station. Seven of these samples were classified, and only one sample from Matimba Power Station (TMT-01), was unclassified. Classified fly ash refers to coal ash whose particles were classified according to its density and aerodynamic as well as magnetic and electrical properties to produce specific fraction of fly ash (Kruger, 1997). The unclassified ash is an agglomerated ash consisting of fine and large particles that were not removed in the flue gases (Ash Resource, 2012).

Table 4.1: List of all fly ash samples collected for CO_2 sequestration

Power station	Sample ID	Particle size from the company
Lethabo	TL-01	97% < 10 µm
Lethabo	TL-02	97% < 10 µm
Lethabo	TL-03	85% < 45 µm
Lethabo	TL-04	80% < 200 µm
Matla	TM-01	95% < 10 µm
Matla	TM-02	85% < 45 µm
Matla	TM-03	85% < 45 µm
Matimba	TMT-01	Unclassified

Prior to conducting any experiments, each of these fly ash samples were first sub-divided using a rotary splitter to obtain representative homogeneous sub-samples. The fly ash samples were then characterised using the techniques discussed in section 4.2 and selected for the purpose of this investigation. This was done to better understand how the various properties (e.g. particle size, mineral composition etc) would affect the carbonation of fly ash, and to what extent, and to select the best fly ash for this purpose.

4.2 Characterization of fly ash

X-ray diffraction (XRD) analysis was used to determine the mineral composition of the fly ash. The elemental concentrations and composition were determined using X-ray florescence (XRF). The Brunauer, Emmet, and Teller theory (BET) was used to measure the specific surface area per unit mass, while scanning electron microscopy (SEM) was used to study the morphology and to generate elemental maps (e.g. calcium). Particle Size Distribution (PSD) was used to identify particle size variation of the raw fly ash samples and carbonated sample.

4.2.1 X-ray Powder Diffraction (XRD)

X-ray Diffraction (XRD) analyses were performed using the British Standard for non destructive testing of polycrystalline and amorphous materials (XRD: BS EN 13925-2003). XRD is a powerful technique that is used to identify crystallographic structure, chemical composition and physical properties of crystal solid material. XRD measurements were carried out on fly ash and synthesised calcium carbonate samples using a BRUKER D8 ADVANCE instrument coupled with 2.2kW Cu long fine focus tube (Cu Kα, λ=1.54060) and 90 sample position changer. It is equipped with a LynxEye detector with 3.7º active area. . Samples are scanned from 2 to 70° 2θ at a speed of 0.02° 2θ steps size/3 sec, and generator settings of 40 kV and 40mA.

The powdered crystalline samples (i.e. calcium carbonate) were first grinded gently using mortar and pestle. The sample was then homogenised to get a representative sub-sample. The sub-sample was mounted into a shallow plastic sample holder against a rough filter paper to ensure random orientation

For the quantification of the amorphous phase untreated and treated fly ash samples were prepared by weighing 0.9 g of sample and 0.1 g of zinc oxide (ZnO). 10 ml of ethanol was added and the sample was placed in a McCrone micronizing mill to reduce the particle size to approximately 5-10 μm in size. The ZnO was added as an internal standard in order to quantify the amorphous phases. Once a sample was micronized, it was transferred into a watch glass and dried overnight at 40 °C in an oven. A sub-sample was pressed into a shallow plastic sample holder against a rough filter paper to ensure random orientation and analysed.

The BRUKER DIFFRAC^{Plus} - EVA evaluation program was used for identification of the mineral phases present in the sample. The ICDD (JCPDS) Inorganic/Organic Database was used for phase search, of which the PDF- 2, release 2006 is available. To quantify the XRD analyses, the Rietveld method was performed using DIFFRAC^{Plus} – TOPAS software with accuracy in the region of ±1%. The structure databases used were the Inorganic Crystal Structure Database (ICSD), the Cambridge Structure Database (CSD) or the TOPAS Structure Database provided by the instrument/software supplier.

4.2.2 X-ray Fluorescence (XRF)

XRF was used for the analysis of major elements in the fly ash samples. Since the particle sizes of fly ash sample were less than 75 μm, there was no need for milling. The fly ash sample was roasted at 1000 °C for at least 3 hours to oxidise Fe^{2+} and S, until the mass of the sample ceased to change. The difference of the unoxidised sample to the stage where all the volatiles are released and the mass of the sample does not change is referred to as the loss on ignition (LOI). Glass disks were prepared by fusing 1.5 g roasted fly ash and 9 g flux consisting of 35% $LiBO_2$ and 65% $Li_2B_4O_7$ at 1000 °C. The samples were analysed using a PANalytical Axios X-ray fluorescence spectrometer equipped with a 4 kW Rh tube.

4.2.3 Scanning Electron Microscopy (SEM-EDS)

SEM-EDS was used to collect micrographs of the fly ash samples and of the formed carbonated products and to complement the XRD results. These analyses were performed using a Leica Stereoscan 440 SEM linked to an OXFORD INCA EDS (Energy Dispersive System). The instrument is equipped with an Oxford X-Max SDD detector with 20 mm^2 active area and a resolution of ca. 128 eV for Mn Kα (5895 eV). This system is able to produce Secondary Backscattered and Cathodoluminescence Electron Imaging, X-Ray EDS microanalysis and X-Ray element mapping.

Fly ash samples were mounted on carbon tape and coated with either carbon or gold to provide a conductive surface for optimum imaging and X-ray microanalysis. Qualitative chemical compositions were determined by means of spot analyses at beam settings of 20 kV accelerating voltage, a probe current of 5.0 nA and counting time of 100 s. Elemental maps were recorded at the same settings by scanning the beam over a selected area for 1-3 hours.

The default reference standards as supplied by Oxford's INCA software as well as own standards were used for calibration and standardization.

4.2.4 Inductively Coupled Plasma Mass Spectroscopy (ICP-MS)

Inductively Coupled Plasma Mass Spectrometry (ICP-MS) was used to identify and quantify major, minor and trace elements in brines or supernatant samples.

Standard solutions and dilution of samples were done using ultra-pure water (18.2 MΩ) and analytical grade (AR) nitric acid (HNO_3). 20 ppb Indium and 30 ppb Iridium were added to samples and calibration solutions as internal standards, in order to correct for instrument drift. Indium (isotope 115) was used as internal standard to correct the drift in elements with masses between 7 and 130 (Li to Te), while iridium (isotope 193) was used as an internal standard for the heavier elements (Ba to U). The calibration standards were prepared using the MerckVI multi-element standard (containing 30 elements) and single element standard solutions for the major elements and silica.

Dilution factors were chosen such that the sample introduction system does not clog due to high salt concentrations and that it does not saturate the detector, so that the elements can be measured close to the calibration range. A dilution factor of 200 was commonly used.

The analyses of all liquid samples were undertaken using a PerkinElmer SCIEX (Concord, Ontario, Canada) ELAN® 9000 ICP-MS system, coupled with a standard cross-flow nebulizer and a Scott-type Ryton ® double-pass spray chamber. Samples were introduced via a Tygon ® peristaltic pump tubing on a Perkin Elmer AS91 auto-sampler, using a Type F auto-sampler tray with 150 sample positions of 16 ml vials.

4.2.5 Carbon/Sulphur (C&S) analyses

Carbon and sulphur analyses were performed using an Eltra CS 800 Double Dual Range system. Between 50 and 200 mg of milled sample (less than 75 micron) were weighed into a ceramic crucible, in which iron and tungsten chips were added, mixed and then combusted in a stream of oxygen. Carbon, present as carbonate, graphite or organic carbon, and sulphur present as sulphate, sulphide or elemental sulphur, are converted to CO_2 and SO_2 respectively. These gasses are then detected using four infrared absorption detectors. The

instrument was calibrated using certified carbon and sulphur standards (Euronorm-CRM 484-1 Whiteheart malleable iron and Leco No 501-502). The concentration of the unknown sample can then be measured by comparison with calibration curves.

4.2.6 Particle Size Distribution (PSD)

Particle size distribution (PSD) of fly ash and carbonated samples was obtained by laser diffraction (Malvern Mastersizer 2000 fitted with a Hydro 2000G wet dispersion unit, Malvern Instrument Ltd. Worcester, UK). Scattered light data were recorded from 2000 to 5000 snapshots of 10 μs. A polydisperse mode of analysis and a refractive index of 1.533 with an absorption index of 0.1 were chosen. For calcium carbonate samples a refractive index of 1.57235 and an absorption index of 0.1 were selected to analyse these samples. Size data collection was performed at constant obscuration in the range 10–20%. This range was selected because there are few particles below 10% thus the reading is close to the blank, whereas above 20% the sampler gets over concentrated.

4.2.7 Brunauer, Emmett and Teller Theory (BET)

BET analyses were performed on a NOVA e Series from Quantachrome Instruments, USA. Prior to performing gas sorption tests, the fly ash surfaces must be freed from any form of contaminants like water. This process is called surface cleaning, also known as degassing. It was carried out at 350 °C for 3 hours on all fly ash samples. It is conducted by placing a small amount of the solid sample in a glass cell and heating it under vacuum or flowing gas. After all the surface water is removed the sample is brought to a constant temperature by an external heating source. Thereafter, small amounts of a gas are admitted in steps into the evacuated sample chamber. Then nitrogen gas is passed over the powder a monolayer of nitrogen molecules. The adsorbed molecules can be used to estimate the number of molecules required to cover the adsorbent surface. The sample surface area can be estimated by multiplying monolayer adsorbed molecules by the cross-sectional area of an adsorbate molecule.

4.3 Leaching of fly ash in acid solutions with varying concentrations of hydrochloric acid and in ultra pure water

The carbonation of fly ash depends of the availability of Ca, Mg and Fe ions in solution and the rate at which they are released from the solid. Therefore, to understand this concept, three hydrochloric acid solutions with varying concentrations (Table 4.2) and ultra-pure water were used for this purpose. Mixtures containing 20 g of fly ash and 200 ml of solvent was stirred for 60 min at atmospheric pressure. After 60 min, the mixture was centrifuged for 10 min to separate the supernatants from undissolved solids (pellets). The supernatants were analysed using ICP-MS, the pellets were thoroughly washed using ultra-pure water, to prevent any further leaching on the pellets and dried at 40 °C. The supernatants and pellets were subsequently submitted for ICP-MS and XRD analyses, respectively.

Table 4.2: Experimental conditions for leaching

S/L (g/ml)	Solvent	Temp (°C)	Pressure	Duration (min)
20/200	H_2O	44	atm	60
20/200	0.1M HCl	44	atm	60
20/200	0.5M HCl	44	atm	60
20/200	1M HCl	44	atm	60

* atm = atmospheric pressure

4.4 Preparation of the brine

The chemical compositions of the brines of deep (>800 m) saline formations in South Africa are at PetroSA but not publicly available. For this reason the scientific literature was consulted and the composition of the brine from the Oriskany formation (USA) which is also composed of sandstone (Liu et al., 2010), was used for the purpose of this investigation. Synthetic brine was prepared using the method of Liu et al., (2010). The mass of the salts, with the purity shown in Table 4.3, was calculated using equation 4.1. The salts were weighed and dissolved in ultra-pure water. At times the brine solution was simplified by not adding some of the salts. Ca, Mg and Fe salts were left out in order to investigate whether the carbonated ions were from the fly ash or brine.

$$\text{Mass of salt; g} = (\text{Molar mass of salt}/\text{ Molar mass of ion}) \times \text{Target concentration of ion} \times (\text{Volume}/10^6) \quad (4.1)$$

Table 4.3: Concentration of ions and the salt used (Liu, 2010)

Ions	Concentration of Ions (mg/l)	Salts	Salt added (g/l)	Quality grades
Ca	19570	$CaCl_2 \cdot 2H_2O$	71.786	GR for analysis ACS,ISO,Reag,Ph,Eur
K	2225	KCl	4.242	GR for analysis ACS,ISO,Reag,Ph,Eur
Mg	3440	$MgCl_2 \cdot 6H_2O$	23.761	GR for analysis ACS,ISO,Reag,Ph,Eur
Sr	2000	$SrCl_2 \cdot 6H_2O$	6.086	GR for analysis ACS
Na	6966	NaCl	177.08	GR for analysis ACS,ISO,Reag,Ph,Eur
Ba	9	$BaCl_2 \cdot H_2O$	0.006	GR for analysis ACS,ISO,Reag,Ph,Eur
Fe	5	$FeCl_3 \cdot 6H_2O$	0.015	GR for analysis ACS,ISO,Reag,Ph,Eur

4.5 Carbonation experiments

4.5.1 Experimental setup used in carbonation of fly ash

The experiments discussed in the sections below were conducted using the 600 ml 4568 Series Mini Bench Top Reactor (Parr Instrument Co. Illinois, USA) shown in Figure 4.1. This reactor can work up to a maximum temperature and pressure of 350°C and 200 bar, respectively. It can be pressurized either using CO_2 or nitrogen gas, and is equipped with a rupture disc set at 3000 psi (~207 bar). Every part of this reactor that could potentially be exposed to corrosive substances is made of Hastelloy C-276 (i.e. nickel-chromium-molybdenum alloy). The reactor is fitted with two gas inlet valves (connected to a deep tube), one gas outlet valve, also called a pressure release valve, a gas entrainment impeller with hollow shaft, a high torque magnetic drive with additional drive pulley, permitting a speed up to 1700 rpm, a rigid heating quartz fabric mantle kept in an aluminum shell and an internal cooling coil connected to tap water. Parameters such as temperature, pressure and mixing speed are controlled using CalGrafix software that is connected to a Parr 4857 Power Controller and a 4870 Process Controller.

Figure 4.1: High temperature, high pressure Parr reactor connected to a liquid CO_2 pump

The reactor is connected to two CO_2 dispensing lines which can be selected individually using a three way valve to feed the reactor, and a third line (nitrogen line, green), as depicted in Figure 4.2. The CO_2 concentration can be kept constant in the reactor by combining any of the CO_2 lines with the nitrogen line, where nitrogen line is used to vary the pressure. The pressure from the nitrogen line is up to 200 bar and the gas dispensing CO_2 cylinder (blue) is 55 bar, controlled by means of a pressure–reducing valve. The liquid dispensing CO_2 cylinder (red) is used for all pressures above 55 bar. This system is connected to a liquid boosting pump (MS-36 Series Pump, Haskel International, Inc., USA), which produces pressures up to 310 bar.

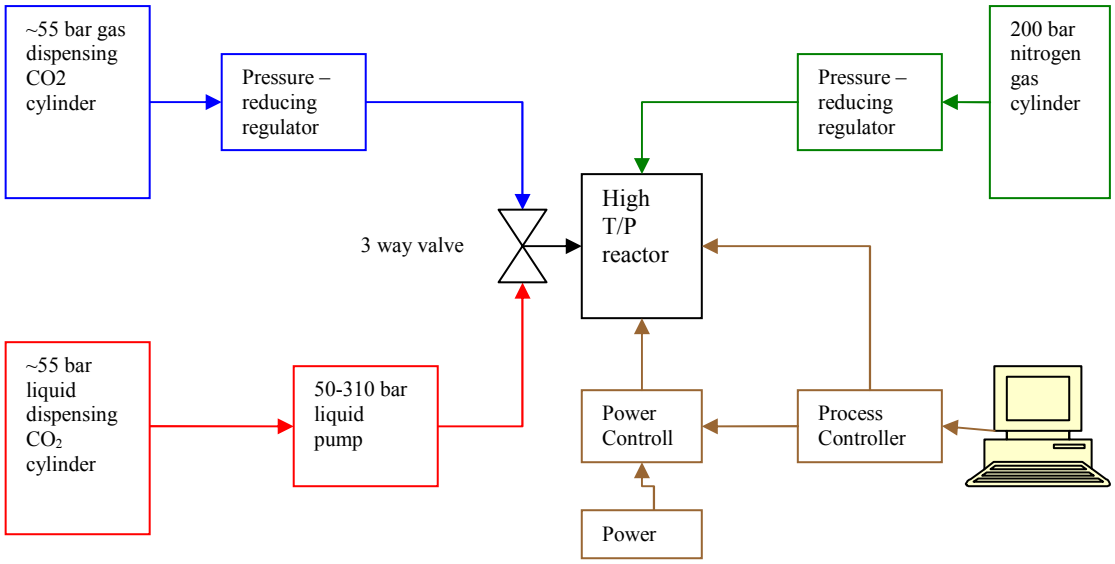

Figure 4.2: Representation of the entire system connected to the reactor

4.5.2 Carbonation of simplified brine

The experiments presented in this section serve to demonstrate hypothesis 1: CO_2 can react with synthetic saline brine under supercritical conditions to form stable mineral carbonates when the pH is adjusted to above 8 by adding sodium hydroxide (NaOH). This is because alkaline conditions (pH above 8) are required for carbonation to take place.

Sodium and calcium are dominant ions in the brine solution. Therefore the initial carbonation experiment involved the carbonation of brine solution containing salt with only these two ions plus chloride since calcium from the brine can react with CO_2 to form carbonates. This brine had a pH 5.73, and about 1.20 g of NaOH was added to 200 ml of the brine solution to increase the pH above 9. This was done for all experiments that involved brine carbonation reaction. The carbonation was undertaken either by adding CO_2 or sodium bicarbonate ($NaHCO_3$) under the following T/P conditions (Tables 4.4 and 4.5): 90 °C/40 bar, 40 °C/90 bar and 90 °C/90 bar, while stirring for 2 hr. Sodium bicarbonate was used at times instead of CO_2 gas to test the effect of CO_2 dissolution in brine has on carbonation. The system was pressurised using nitrogen gas for all carbonation experiments where sodium bicarbonate was used. After 2 hr, the mixture was centrifuged for 10 min to separate the liquid (supernatant) from the solids (pellets). After separation of the supernatant from undissolved solids about 10% by volume of nitric acid was added to the supernatant to

prevent after-effect carbonation, and the resulting solution was stored in a refrigerator, until it was analysed using ICP-MS. The pellets were washed thoroughly using ultra-pure water to remove all the water soluble salts, dried at 40 °C, and analysed by XRD.

Table 4.4: Carbonation experimental conditions using CO_2 gas

Volume (ml)	Temperature	Pressure	Duration
200	90˚C	40bar	120 minutes
200	40˚C	90bar	120 minutes
200	90˚C	90bar	120 minutes

Table 4.5: Carbonation experimental conditions using sodium bicarbonate

Volume	Temperature	Pressure	Duration
200	40˚C	90bar	120 minutes

4.5.3 Carbonation of fly ash

Carbonation of fly ash was conducted either by adding CO_2 or sodium bicarbonate ($NaHCO_3$) under different conditions, as presented in the relevant sections below. At the end of the experiment and upon centrifuging for 10 min, the supernatant was sampled and 10% by volume of 69% nitric acid was added and analysed by ICP-MS. The pellets were washed thoroughly using ultra-pure water, dried at 40 °C, and analysed by XRD.

Three types of solvents were used to prepare the fly ash slurry, namely ultra-pure water, “full synthetic brine” (containing all salts presented in Table 4.3) and “simplified brine” (containing only NaCl and $CaCl_2 \cdot 2H_2O$ salts).

4.5.3.1 Carbonation of fly ash in ultra pure water

These experiments were carried out following the assumed geothermal gradient for South African deep saline reservoirs (Figure 4.3, graph A), as described by Viljoen (2010). The CO_2 density with respect to depth was obtained from Bachu (2003) (Figure 4.3, graph B).

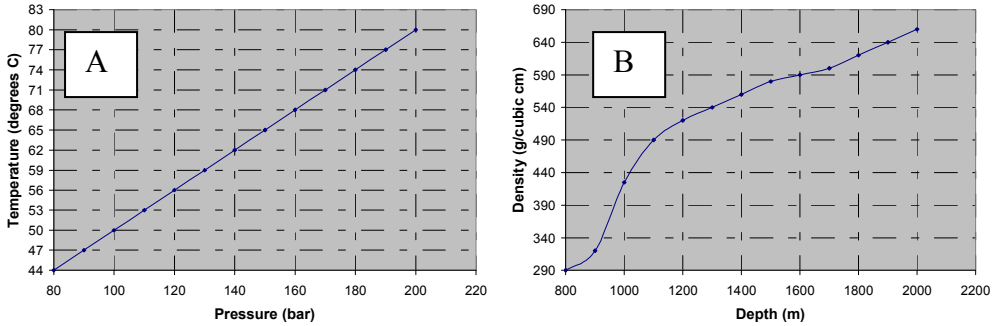

Figure 4.3: graph A: Temperature and gradient; graph B: Change in sc-CO_2 density below 800 m depth (Viljoen, 2010) and (Bachu, 2003)

The fly ash slurry was prepared by adding 40 g fly ash into 400 ml ultra pure water. This slurry was stirred at a constant speed (mark 2 on Parr 4875 power controller) under the experimental conditions presented in Table 4.6.

Table 4.6: Experimental conditions used for carbonation of fly ash in ultra pure water

S/L (g/ml)	Solvent	Temp (°C)	Pressure (bar)	Duration
1/10	H_2O	44	80	60 min
1/10	H_2O	50	100	60 min
1/10	H_2O	44	80	7 days
1/2	H_2O	44	80	7days
1	H_2O	90	50	3 days
1	H_2O	90	50	2 hr
1	H_2O	90	90	2 hr
1	H_2O	90	50	48 hr

4.5.3.2 Carbonation of fly ash in full and simplified synthetic brine

The suspension was prepared using 200 ml synthetic brine and 200 g fly ash. The brine was prepared as in section 4.4 and contained all the salts listed in Table 4.3, and was used to carbonate fly ash under the conditions given in Table 4.7a. The other brine only contained

NaCl and $CaCl_2 \cdot 2H_2O$ salts was used in the carbonation of fly ash under conditions given in Table 4.7b. The mixtures were stirred at a constant speed for 2 hr.

Table 4.7a: Experimental conditions used for carbonation of fly ash in full brine

S/L (g/ml)	Brine	Temperature (˚C)	Pressure (bar)	Duration (min)
1	All salts*	90	50	120
1	All salts*	90	70	120
1	All salts*	90	90	120

*as listed in Table 4.3

Table 4.7b: Conditions used for carbonation of fly ash in Simplified brine

S/L (g/ml)	Brine	Temperature (˚C)	Pressure (bar)	Duration (min)
1	NaCl + $CaCl_2$*	90	40	120
1	NaCl + $CaCl_2$*	90	70	120
1	NaCl + $CaCl_2$*	90	90	120

*concentrations listed in Table 4.3

At the end of the experiment and upon centrifuging for 10 min, 1.4 ml of the supernatant was transferred into a 1.6 ml centrifuge tubes and 0.14 ml of nitric acid was added to each centrifuge tube in order to lower the pH, i.e. preventing carbonation. These samples were then analysed by ICP-MS. The pellets were rinsed three times with ultra-pure water and left to dry in an oven at 40˚C, until a constant weight was reached, after which XRD analyses were performed.

CHAPTER FIVE
RESULTS AND DISCUSSION

5.1 Characterization of fly ash samples

The particle size distribution (PSD) was used to verify the PSD data obtained from industry for these samples. From these analyses five samples were shortlisted. Sample TM-01 was discarded because of its high silica-fume content (Kruger, 2010); resulting in repetitive variation of PDS results (see Table 5.1). The data obtained from the industry was slightly different from the one obtained using Malvern Mastersizer 2000. This could be as a result of difference in analytical techniques. The technique used in the industry is not known at this stage. Sample TM-03 and TL-02 were also discarded because it was identical to sample TM-02 and TL-01 respectively, the only difference being that it was sampled on a different date. The PDS of these samples shown as peaks in Figure 5.1 are somewhat identical, suggesting little or no different in terms of particle size range.

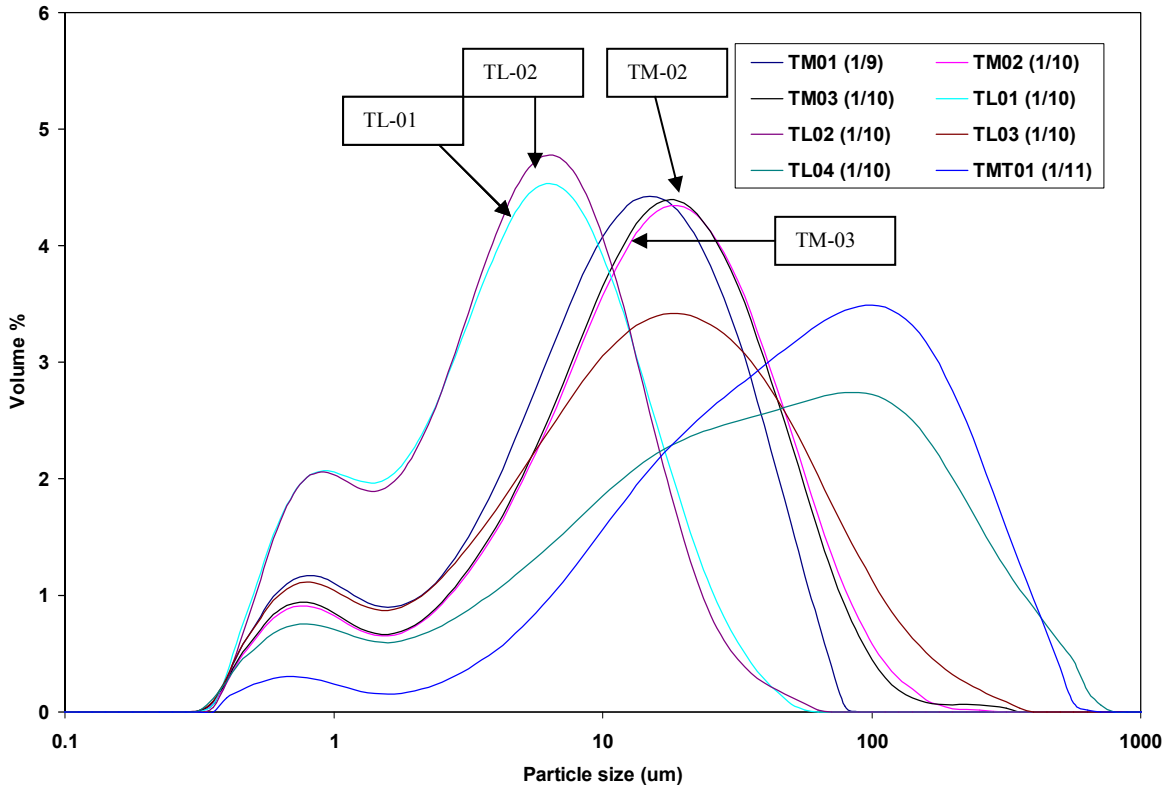

Figure 5.1: Particle size distribution for all untreated fly ash samples with overlapping peaks

Table 5.1: List of all fly ash samples collected for CO_2 sequestration

Power Station	Sample I.D.	data from the industry	Malvern Data	Comment
Lethabo	**TL-01**	97% < 10µm	79% < 10µm	only sample used
Lethabo	**TL-02**	97% < 10µm	80% < 10µm	discarded
Lethabo	**TL-03**	85% < 45µm	84% < 45µm	
Lethabo	**TL-04**	80% < 200µm	D(v,0.8) = 124.3 ± 4.8 D(v,0.9) = 205.0 ± 7.4	
Matla	**TM-01**	95% < 10µm	48% < 10µm	discarded
Matla	**TM-02**	85% < 45µm	89% < 45µm	
Matla	**TM-03**	85% < 45µm	90% < 45µm	discarded
Matimba	**TMT-01**	Unclassified	89% < 200µm	

The PSD data were then compared to surface area (Figure 5.2). The classified samples (in a yellow box) have smaller diameter and a large surface area per unit mass. These samples are expected to have increased reactivity as oppose to the unclassified samples. However, TL04 has a large surface area per unit mass though its particles are large. This sample and TMT-01 were eliminated because their particles are too large (Table 5.2) to be injected with CO_2 into a storage reservoir.

Table 5.2: PSD and surface area per unit mass of untreated fly ash

Sample ID	BET (m^2/g)	D(v,0.1)	D(v,0.5)	D(v,0.9)	D[3,2]	D[4,3]
TMT-01	0.738	7.43	52.51	216.53	11.85	86.26
TL-03	1.095	1.3	13.6	63.6	4.0	27.3
TM-02	1.496	1.8	13.9	46.8	4.5	20.4
TL-01	1.515	0.83	4.61	14.87	2.31	6.57
TL-02	1.528	0.86	4.60	13.78	2.37	6.33
TL-04	1.790	2.3	33.9	205.0	5.8	75.2

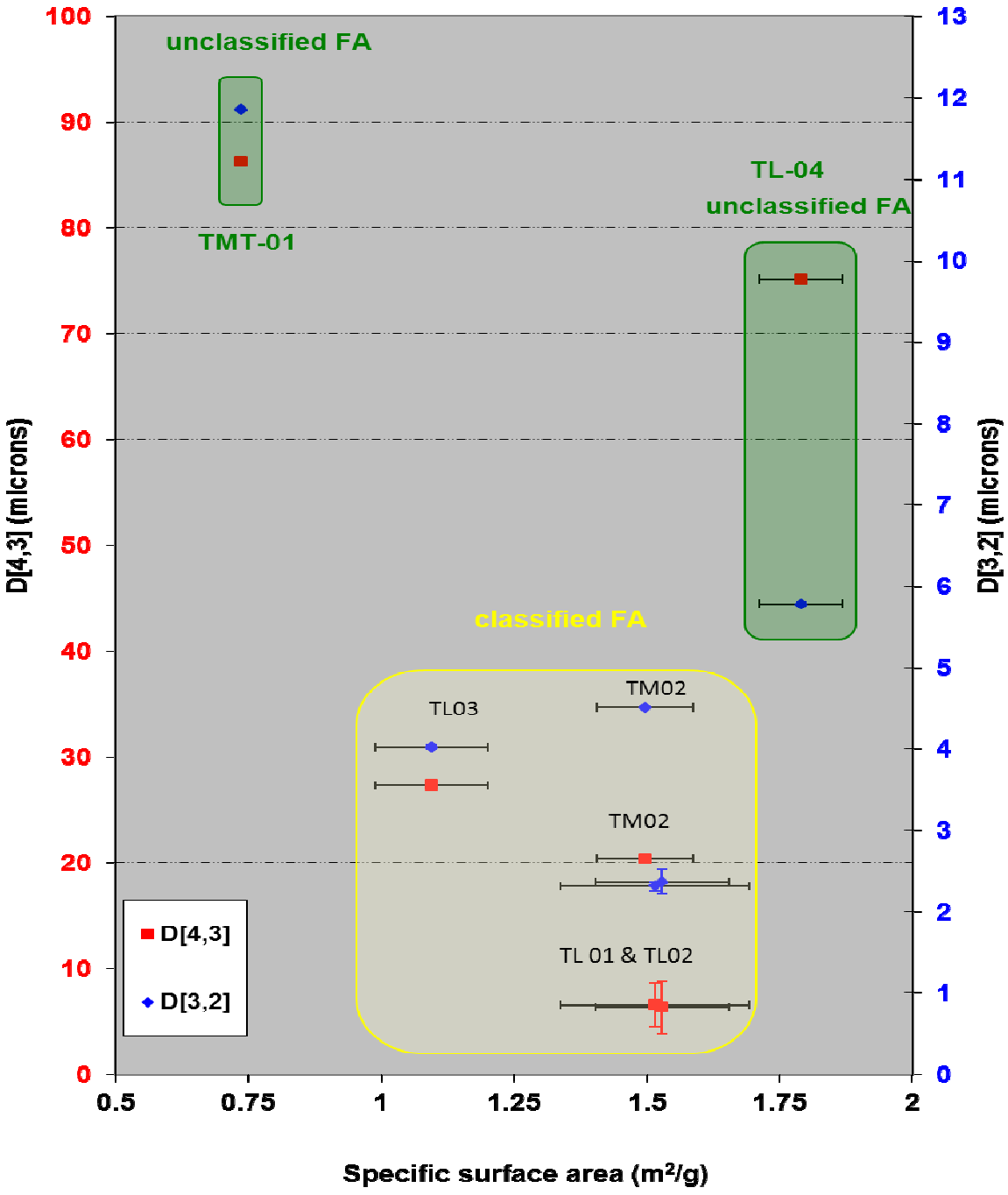

Figure 5.2: Relationship between particle size and surface area

Fly ash TL-01 best fits the requirement to inject into a saline reservoir with CO_2 since it has the smallest particle size distribution and contains 5.27% CaO that was not identified in any mineral phases (Table 5.3). TM-02 is also a good candidate for this purpose since it has high CaO but its particle may be too large to be pumped through the pores.

Table 5.3: XRF results for the six shortlisted fly ash samples (wt%)

Sample ID	TL-01	TL-02	TL-03	TL-04	TM-02	TMT-01
SiO_2	52.09	52.16	55.41	55.79	50.52	59.73
TiO_2	1.79	1.78	1.69	1.63	1.74	1.27
Al_2O_3	33.17	33.17	31.3	30.25	32.22	25.86
Fe_2O_3(t)	3.34	3.41	3.28	3.43	3.12	6.67
MnO	0.04	0.04	0.03	0.03	0.03	0.07
MgO	1.33	1.31	1.13	1.1	1.73	0.85
CaO	5.27	5.23	4.82	4.88	6.92	2.92
Na_2O	0.26	0.29	0.24	0.22	0.6	0.11
K_2O	0.99	1.02	0.95	0.86	0.73	0.95
P_2O_5	0.68	0.7	0.51	0.4	0.91	0.42
Cr_2O_3	0.04	0.04	0.04	0.03	0.03	0.02
L.O.I.	0.51	0.48	0.37	0.74	0.96	0.85
Total	99.52	99.61	99.76	99.38	99.52	99.73

Further characterization was performed using XRD (Table 5.4), which showed no or little minerals that usually contain Ca, Mg and Fe as their main component. These three elements are mostly considered for mineral carbonation and were only detected using XRF. A conclusion was made that these element occur either in the amorphous phase or as trace elements in minerals like feldspar or anhydrite.

Table 5.4: Mineralogical composition of untreated fly ash samples

Sample	Chemical Formulae	TL01	TL02	TL03	TL04	TM02	TMT01
Amorphous Content	_	63.98	63.8	62.14	55.5	61.05	54.12
Anhydrite	$CaSO_4$	trace	trace	trace	trace	1.08	trace
Mullite	Al_2O_3 SiO_2	29.45	30.18	28.81	31.85	28.31	29.44
Quartz	SiO_2	5.88	5.27	8.55	11.94	6.72	12.69
Lime	CaO	-	-	-	-	0.69	trace
Magnetite	Fe_3O_4	-	-	-	-	0.81	2.42
Periclase	MgO	-	-	-	-	1.16	trace
Rutile	TiO_2	trace	trace	trace	trace	trace	trace
Jarosite	$KFe^{3+}_3(SO_4)_2(OH)_6$	trace	-	-	-	trace	trace
Total	-	99.31	99.25	99.5	99.29	99.82	99.78

Fly ash was also studied using SEM and the images presented in Figure 5.3 were captured. These micrographs show the classified "A" (TL-01) and unclassified "B" (TMT-01) fly ash, with the spherical amorphous particles and few agglomerated particles. The spherical amorphous particles indicate that the particles were formed under uncrowded freefall conditions and quenched to maintaining the glassy spherical shapes (Saikia et al., 2006).

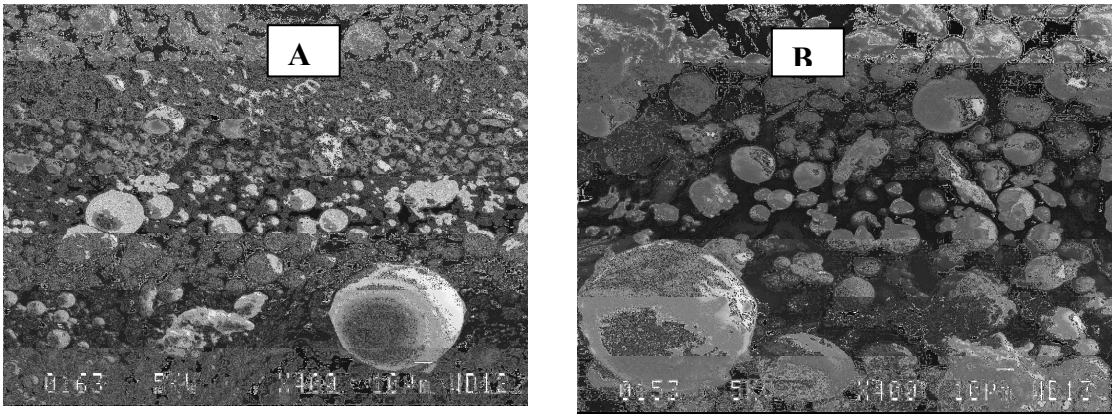

Figure 5.3: SEM image showing the spherical amorphous phase of fly ash classified "A" and unclassified "B"

5.2 Leaching of fly ash in acidic solutions with varying concentrations of hydrochloric acid and in ultra-pure water

The carbonation of fly ash mostly depends on the availability of Ca, Mg and Fe ions in the solution and the rate at which they are released from the solid. In order to test the realized of these ions in solution fly ash was leached in ultra-pure (control) and in three hydrochloric acid solutions with varying concentrations. The mixtures containing fly ash and these solvents had a S:L ratio of 1/10 and were stirred at atmospheric pressure for 60 min. The supernatant was sampled from leaching of fly ash and analyzed using ICP-MS (Table 5.5). These results show that more Ca, Mg and Fe were released under more acidic conditions. The XRD results of the leached material show a significant change in the amount of the amorphous phase (between 6.61-14.73%) when compared to the untreated fly ash (Table 5.6). The detection of corundum (up to 8.28%) under these conditions is not conceivable but it could be caused by contamination from the industry, probably grinding.

Table 5.5: ICP-MS results of liquid component from leaching fly ash

Samples	%Mg released	%Ca released	%Fe released
H_2O	0.05	5.54	0.05
0.1 M HCl	15.43	38.15	0.40
0.5 M HCl	27.65	54.87	13.94
1 M HCl	31.00	63.13	16.75

Table 5.6: XRD results of the solid components from ultra pure water and acid leached fly ash

Content %	untreated	H_2O	0.1 M HCl	0.5 M HCl	1 M HCl
Amorphous Content	63.98	57.37	53.52	49.25	55.52
Quartz	5.88	7.06	7.50	7.52	7.31
Mullite	29.45	33.78	38.19	34.00	34.01
Rutile	trace	trace	trace	Trace	trace
Calcite	-	trace	-	-	-
Anhydrite	trace	trace	trace	-	trace
Magnetite	-	-	-	-	-
Periclase	-	-	-	-	-
Jarosite	trace	-	-	-	-
Corundum	-	1.05	-	8.28	2.40
Total	99.31	99.26	99.21	99.05	99.24

5.3 Carbonation of simplified brine

The experimental conditions for this section are discussed in section 4.5.2. These experiments were designed to investigate the carbonation of brine under sc-CO_2 conditions and to obtain the conditions with the best yield. At end of the experiment, the pellets that were obtained by centrifugation and separated from supernatant were dried at 40°C and subsequently weighed before analysis. The white powdery solids formed when using CO_2 gas weighed between 1.09 g and 1.31 g. These formed powder were essentially composed of calcite (>99% $CaCO_3$), as illustrated by XRD (Table 5.7). By taking into account the amount of calcium in untreated brine and the amount of calcium in the formed $CaCO_3$, it can be estimated that about 11.17 and 13.44% of the total calcium from the brine was converted to carbonates under the experimental conditions of this study (Table 5.8).

The traces of dolomite, mullite and quartz are the result of fly ash contamination from previous work which stuck on the walls of the reactor and it was difficult clean. Dolomite was not expected because there was not Mg in the salts that were used to prepare the brine. There was also about 0.76 g of wollastonite detected due to quartz contamination from fly ash.

Table 5.7: Sample yields from carbonation of simplified brine (composed of NaCl and $CaCl_2$) through CO_2 gas (pH 9) for 2 hours

T/P Conditions	Mass yield (g)	Wollastonite	Dolomite	Calcite	Mullite	Quartz
-	-	$CaSiO_3$	$CaMg(CO_3)_2$	$CaCO_3$	$Al_6Si_2O_{13}$	SiO_2
40 °C/90 bar	1.19	0.76	Trace	99.16	Trace	trace
40 °C/90 bar	1.09	trace	Trace	99.8	Trace	trace
90 °C/40 bar	1.31	trace	Trace	99.81	Trace	trace
90 °C/40 bar	1.21	trace	Trace	99.86	Trace	trace
90 °C/90 bar	1.22	trace	Trace	99.77	Trace	trace
90 °C/90 bar	1.17	Trace	Trace	99.79	trace	trace

Table 5.8: Amount of Ca in the brine that reacted with CO_2 under the different experimental conditions

T/P Conditions	Starting Ca g/200ml	Ca reacted (g)	%Ca reacted
40 °C/90 bar	3.91	0.48	12.17
40 °C/90 bar	3.91	0.44	11.17
90 °C/40 bar	3.91	0.53	13.44
90 °C/40 bar	3.91	0.49	12.42
90 °C/90 bar	3.91	0.49	12.47
90 °C/90 bar	3.91	0.47	11.97

Since the CO_2 injection into the deep saline reservoir is expected to take place at depth of >800 m and not more than 2000 m, and the conditions 40 °C and 90 bar are close to the expected the T/P conditions in the saline reservoir within this depth. Therefore, these conditions were also used for the experiment with sodium bicarbonate in place of CO_2 gas. An interesting observation was made that if sodium bicarbonate is used, the calcium carbonate yield increases by a factor of six (Figure 5.4, Table 5.9). Hence 64% of Ca in solution reacted to form carbonate within the same duration (i.e. 2 hr) and T/P condition when compared to using CO_2 gas above. This observation can be explained in terms of the dissolution of CO_2 in brine, which is the rate limiting factor (discussed in Chapter 6).

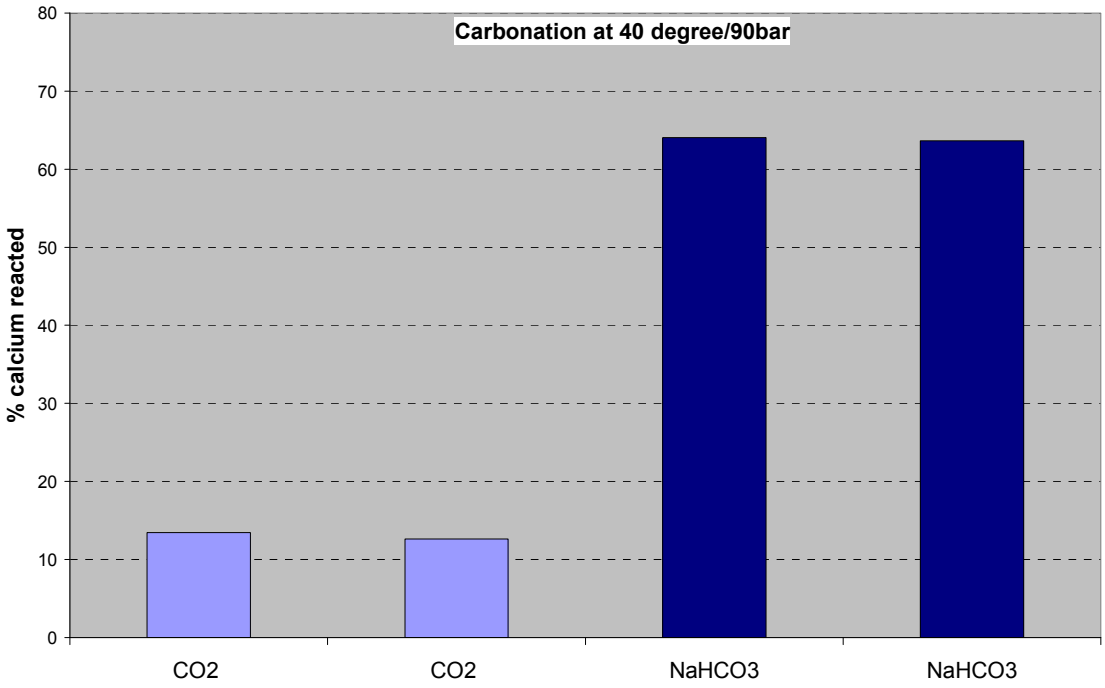

Figure 5.4: Comparison between the calcium ions that reacted when using CO_2 gas and Sodium bicarbonate at 40 °C and 90 bar

Table 5.9: Yield of formed product from carbonated brine using sodium bicarbonate as source of CO_2

Conditions	mass yield (g)	Calcite	Halite*	Ca reacted (g)	%Ca reacted
40 °C/90 bar	6.25	100	0.00	2.50	64.03
40 °C/90 bar	6.22	99.34	0.66	2.49	63.65

* NaCl

ICP-MS could not be used for estimating the unreacted Ca for comparison with calculated XRD derived values due to highly concentrated in sodium ions, which interfered with the plasma. In order to confirm the effect that sodium ions has on the ICP-MS result obtained for the concentration of Ca, a short explorative experiment was performed where the concentration of calcium ions in solution was kept constant for all samples, but the sodium ion concentration was varied with dilution factors of 0, 2, 5, 10 and 100. The ICP-MS result presented in Figure 5.5 shows that at lower sodium concentration the measured values for sodium are closer to theoretical values than at higher concentrations. A similar observation was made with calcium ions (Figure 5.6), where the calcium concentration is closer to the theoretical values at lower sodium concentrations than at higher sodium concentration.

Table 5.10: Comparison of calculated percentage of unreacted calcium from ICP-MS and XRD results of the experiment with high sodium concentrated brine which interfered with the plasma

T/P Conditions	%Ca unreacted from ICP-MS	%Ca unreacted from XRD	Sodium*
40 °C/90 bar	74.68	25.32	S
40 °C/90 bar	73.57	26.43	S
90 °C/40 bar	76.94	23.06	S
90 °C/40 bar	75.17	24.83	S
90 °C/90 bar	78.76	21.24	S
90 °C/90 bar	76.58	23.42	S

*ICP-MS detector saturated (S)

The carbonates discussed in this section were formed from the brine that contains NaCl and $CaCl_2 \cdot 2H_2O$ salts. Therefore, only calcium carbonates were expected in this scenario. This was confirmed with XRD which detected almost 100% $CaCO_3$ and weight of the product after drying is known. If the initial concentration of Ca in brine and its percentage in $CaCO_3$ is known the amount of Ca unreacted can therefore be calculated. Similarly, if the concentration of Ca in the supernatant (from ICP-MS) and the initial concentration are known the amount of Ca unreacted can be calculated.

Figure 5.5: The measured sodium concentration values deviates from the real value as the brine become more concentrated in sodium

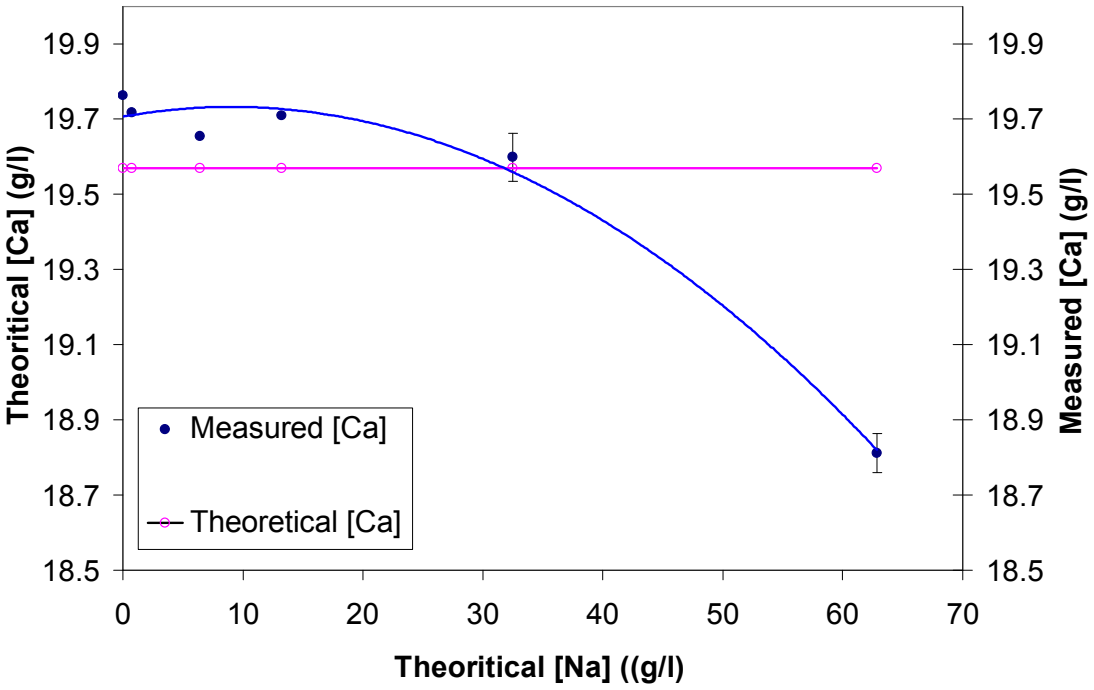

Figure 5.6: Calcium concentration values are more accurate at lower sodium concentrations than at higher sodium concentrations

The calcium carbonate samples were further analysed to determine their particle size distributions. The carbonates produced using CO_2 gas are much finer compared to the samples formed using sodium bicarbonate (Figure 5.7) though they were formed under the same experimental conditions (90 °C/40 bar). The sample formed using CO_2 gas has D(v,0.9) of 4.85 µm meaning that 90% of the volume distribution has a diameter that is less than 4.85 µm, whereas samples produced using sodium bicarbonate has D(v,0.9) of 40.11 µm.

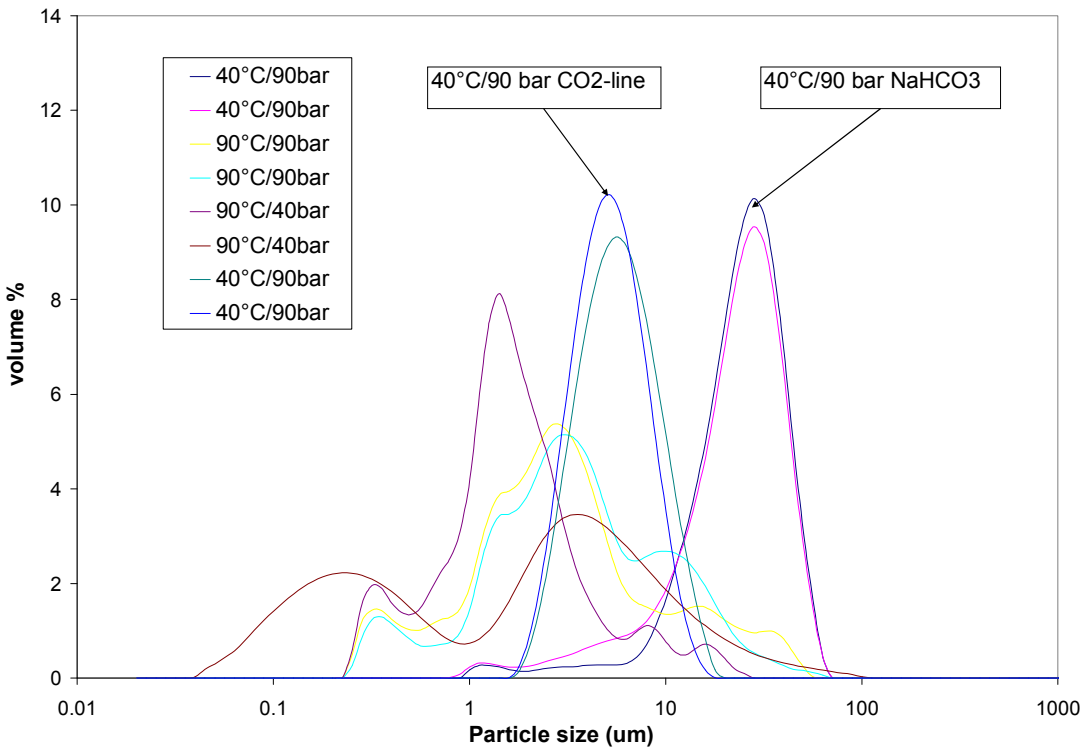

Figure 5.7: Particle size distribution of carbonates formed from simplified brine using CO_2 gas and sodium bicarbonate

The observation in Figure 5.7 was confirmed by SEM analyses (Figures 5.8 and 5.9). Figure 5.8A shows a general particle size distribution of the carbonates formed using sodium bicarbonate. The morphologies of calcium carbonates (Figure 5.8B and C) were studied using secondary electrons. These particles shown in Figure 5.8B and C have a well defined growth plane.

The carbonate particles produced by using the CO_2 gas are much finer (Figure 5.9A) than carbonate particles formed with sodium bicarbonate (Figure 5.8A) because of the rate limiting dissolution of CO_2 in the brine was avoided in the sodium bicarbonate experiment. Therefore, the kinetics is much quicker with sodium bicarbonate and the extent of nucleation is much greater. The presence of crystal planes were not confirmed in the case of carbonates formed using CO_2 gas (Figure 5.9) because the analysis was done under electron backscattering mode. The SEM could not focus if the secondary electrons were used because the particles were very fine.

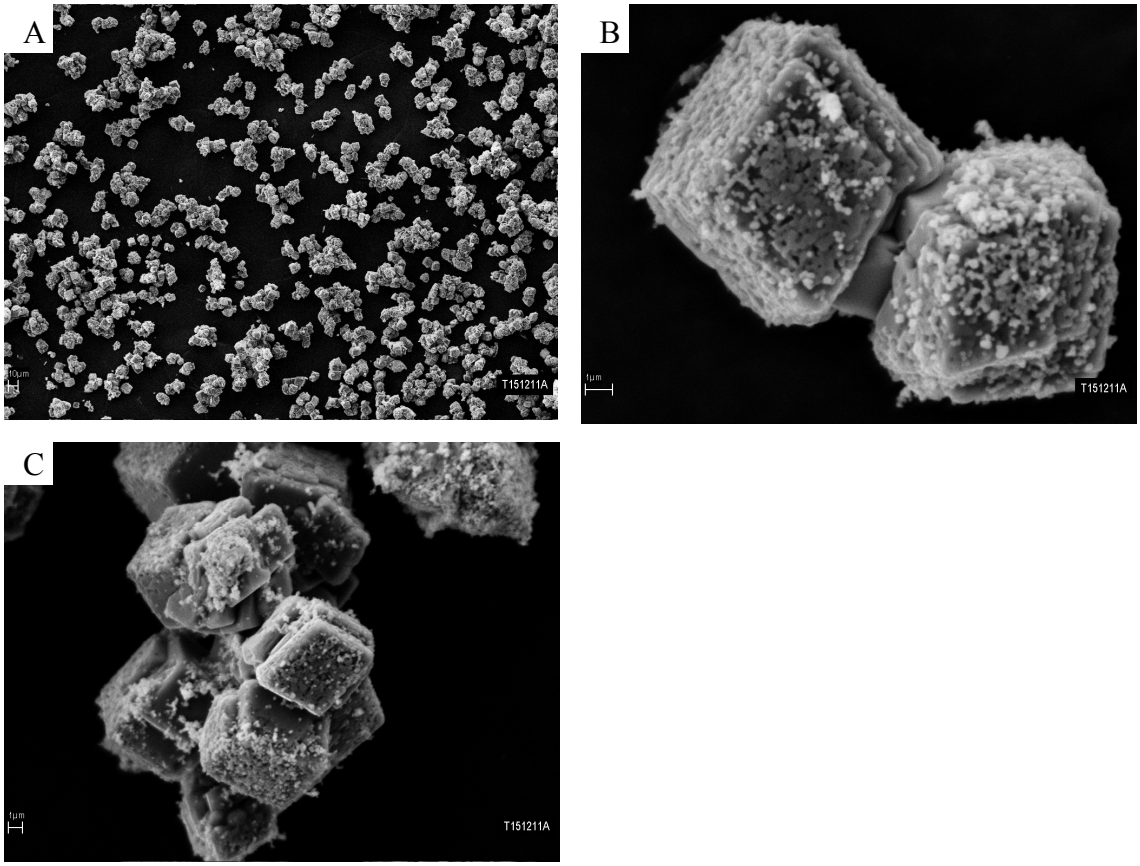

Figure 5.8: Morphology and particle size distribution of carbonates formed using sodium bicarbonate

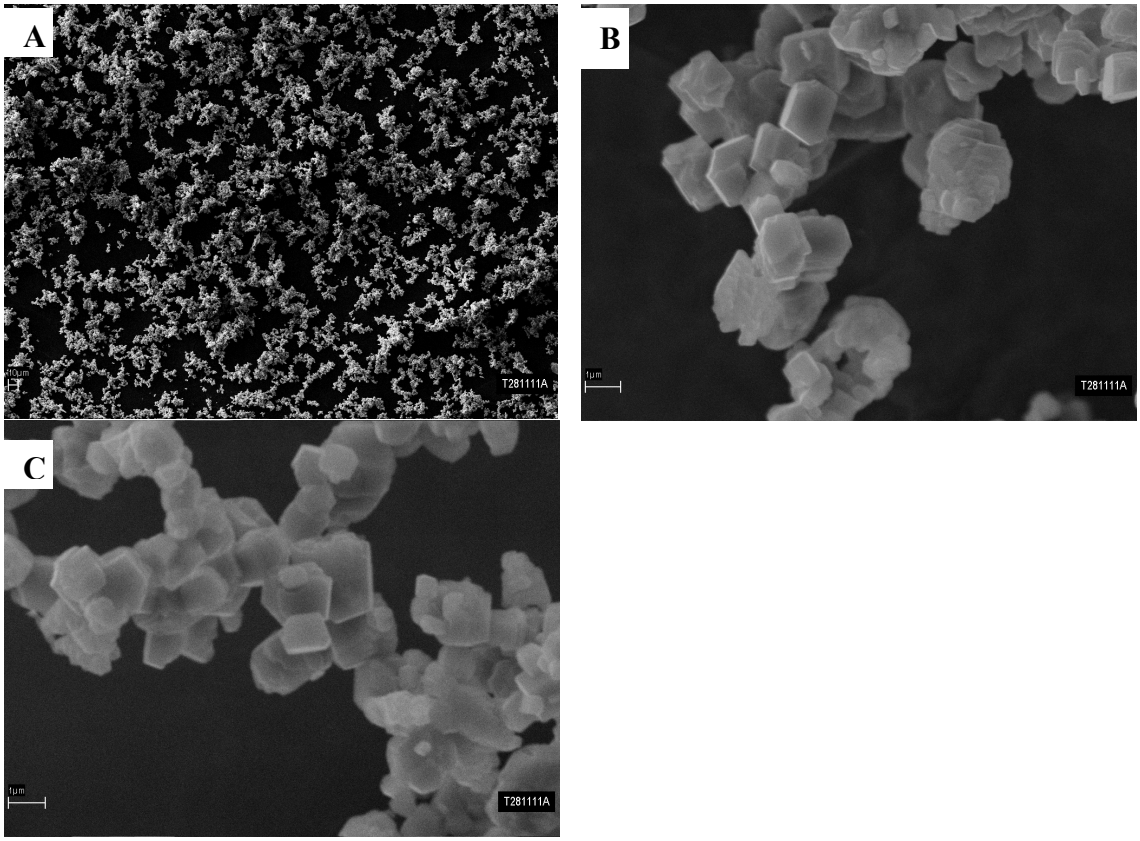

Figure 5.9: Morphology and particle size distribution of carbonates formed using CO_2 gas

Elemental mapping was also performed on the respective carbonates (Figures 5.10 and 5.11). These analyses were performed on an uneven surface of the samples mounted on a carbon tape. The results indicated that there is a small amount of NaCl and $CaCl_2$ in these samples although XRD did not detect it. This conclusion is based on the fact that the only salts present in the brine were NaCl and $CaCl_2 \cdot 2H_2O$. Therefore, in areas where oxygen and calcium is detected the product is most likely to be calcium carbonate. However, where there is absence of oxygen but chlorine and/or sodium occurs together the particles can either be NaCl or $CaCl_2$.

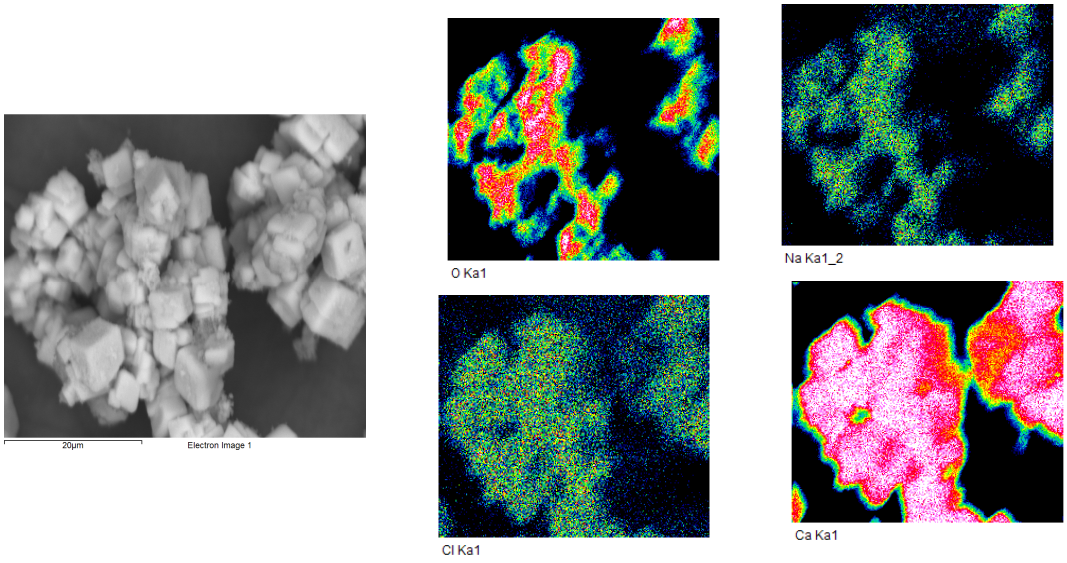

Figure 5.10: Relative elemental distribution of carbonates formed using Sodium bicarbonate as determined by SEM

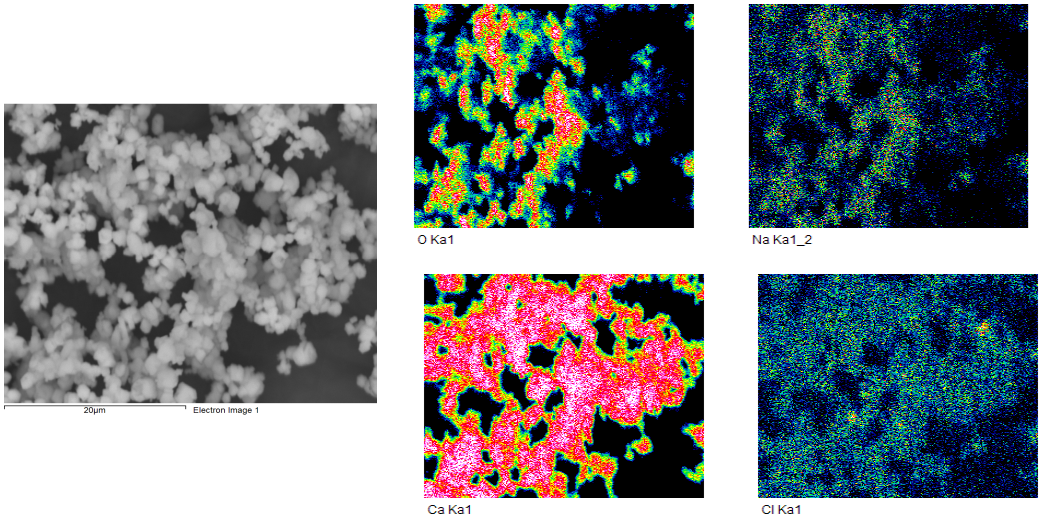

Figure 5.11: Relative elemental distribution of carbonates formed using CO_2 gas as determined by SEM

5.4 Carbonation of fly ash in ultra-pure water

The initial set of experiments were conducted using ultra-pure water as a solvent, as discussed in section 4.5.3.1. All the experiments that were conducted under these conditions, with the duration of 120 min or less (Table 5.11), showed no evidence of carbonation using XRD. Subsequently the experiments were run for a much longer time (Table 5.12). After three days and seven days the results began to show up to 1.78% calcite and traces of aragonite.

Table 5.11: XRD results of fly ash that was treated with CO_2 in ultra-pure water

T/P conditions	**Untreated**	**44/80**	**44/80**	**50/100**
Duration	**-**	**60 min**	**60 min**	**60 min**
Amorphous Content	63.98	59.37	62.89	56.01
Quartz	5.88	7.17	6.30	7.06
Mullite	29.45	32.78	30.53	36.63
Rutile	Trace	trace	Trace	Trace
Calcite	-	-	-	-
Anhydrite	Trace	-	-	-
Jarosite	Trace	-	-	-
Total	99.31	99.32	99.72	99.70

Table 5.12: XRD showing the formation of carbonates for longer experiments

T/P conditions	**44°C/80 bar**	**44°C/80 bar**	**90°C/50 bar**	**90°C/50 bar**
Duration	**7 day**	**7 day**	**3 day**	**3 day**
Amorphous Content	62.44	60.97	60.76	64.36
Quartz	6.68	8.67	7.47	6.67
Mullite	28.54	28.44	30.74	27.45
Aragonite	Trace	Trace	trace	trace
Calcite	0.31	1.78	trace	trace
Anhydrite	-	-	trace	trace
Corundum	1.76	-	-	-
Total	99.73	99.86	98.97	98.48

5.5 Carbonation of Fly Ash in brine depleted of Ca, Mg and Fe ions using sodium bicarbonate

The results presented in Table 5.13 are colour-coordinated. They were conducted at conditions as described in Table 5.13, where R-T = room temperature, A-p = atmospheric pressure, FA = fly ash and Bic = sodium bicarbonate. The experimental conditions where sodium bicarbonate was used are indicated with Bic. The brine used in these experiments contained no Ca, Mg or Fe ions. Therefore, all the calcium that would have reacted to form calcite is from the fly ash. The pH of the supernatant was measured at the end of the experiment and ranged between 8.13 and 10.90. The pH values in Table 5.13 are favourable for the formation of carbonates since they are above pH 8. The fly ash slurry prepared with the brine without Ca, Mg and Fe ions was treated with sodium bicarbonate. The yellow and blue columns show significant amount, between 1.76 and 2.30 wt%, of calcite and traces of halite for fly ash samples that were treated with sodium bicarbonate. On the other hand, in the last four columns (red, white and green) where sodium bicarbonate was used only traces of calcite were detected with high concentrations of halite. The high concentrations of halite could possibly the reason for the latter. This observation was verified in section 5.6.

Table 5.13: Other minerals which were detected in carbonated fly ash samples by XRD

Eeperimental conditions	**Unreacted Fly ash**	R-T/A-P 1hr	R-T/A-P 1hr Bic	R-T/60bar 2hr Bic	R-T/100bar 2hr Bic	90°C/A-P 1hr Bic	90°C/A-P 2hr Bic	90°C/60bar 2hr Bic	90°C/100bar 1hr	90°C/100bar 2hr Bic
pH	-	10.65	8.13	8.35	8.32	10.90	8.71	8.70	10.90	8.90
Amorphous Content	63.98	64.63	60.64	60.45	63.11	60.19	63.94	65.43	64.07	61.66
Quartz	5.88	6.58	7.30	7.30	6.50	7.64	6.51	6.01	6.86	6.98
Mullite	29.45	27.50	29.83	29.83	28.35	27.34	26.40	24.37	28.38	28.37
Rutile	Trace	-	trace	Trace	-	-	-	-	-	-
Calcite	-	-	2.30	1.93	1.76	trace	trace	trace	-	trace
Anhydrite	Trace	-	-	-	-	-	-	-	-	-
Halite	-	1.00	trace	Trace	trace	4.30	2.36	3.36	trace	1.74
Jarosite	Trace	-	-	-	-	-	-	-	-	-
Totals	99.31	99.71	100.07	99.51	99.72	99.47	99.21	99.17	99.31	98.75

5.6 Carbonation of fly ash in brine containing only NaCl, using sodium bicarbonate

It was observed in section 5.5 that calcite can be detected when sodium bicarbonate is added into fly ash suspension. Here, the first evidence in this study was observed, of carbonates that were formed under supercritical condition within 2 hr. A significant amount of calcite was formed (~2%, Table 5.13) by improving the dissolution of CO_2 in brine. The experimental condition in Table 5.14 column-A, fly ash and brine were kept stirring for 2 hr prior to adding sodium bicarbonate and leaving it to react for two more hours. For the experiments reported in Table 5.14 column-B, sodium bicarbonate was added to fly ash slurry without the process of leaching. Both of these conditions produced almost the same amount of calcium carbonate.

Table 5.14: Carbonates formed using sodium bicarbonate instead of CO_2 gas

Phase	Formula	44°C/90 bar (A)	44°C/90 bar (A)	44°C/90 bar (B)	44°C/90 bar (B)
Quartz	**SiO_2**	9.07	7.29	8.45	9.72
Mullite	**$Al_6Si_2O_{13}$**	29.96	31.90	27.92	31.38
Calcite	**$CaCO_3$**	2.01	1.97	1.98	2.19
Halite	**NaCl**	Trace	Trace	Trace	Trace
Amorphous Content	-	58.53	58.40	61.32	56.18

5.7 Carbonation of fly ash in full brine

Herein, brine containing all the ions discussed in section 4.6 was used with CO_2 gas not sodium bicarbonate. The carbonation reaction of fly ash with sc-CO_2 was tested in the synthetic brine at T/P conditions of 50 ºC/90 bar and 90 ºC/90 bar, for 2-hours. At the end of the 2-hours contact time, and upon centrifugation and drying of the solid residue at 40 ºC up to constant weight, the residue was examined under a scanning electron microscope (Figures 5.12, 5.13 and 5.14). While a large number of fly ash particles appeared to be intact, fragments of carbonated sheets with widths of *ca.* 3.8 µm were also observed (denoted "$CaCO_3$" in Figure 5.12). The surface of a carbonated sheet is depicted in Figure 5.13. These sheets were enriched in calcium, carbon and other elements i.e. Al, Si, Na, Mg and Cl (Figure 5.14). It is not clear whether the other elements identified in the spectrum are part of the sheet composition or are indicative of an effect of analytical volume created by the SEM

electron beam being larger than the thickness of the sheet. Small amounts of sulphur were also detected. Fly ash particles as well as a small number of needle-shaped gypsum crystals were also embedded in the sheet.

The mineralogical composition of the carbonated sheet was investigated using XRD (Table 5.15), which demonstrated the presence of aragonite (23%), calcite (3%) and fly ash minerals (e.g. mullite, quartz). It also contained an XRD-amorphous phase of about 37%. The carbonated sheet illustrated in Figure 5.12 was most certainly a fragment of a larger sheet which formed at and coated the bottom of the high-pressure, high-temperature reactor (Figure 5.15). The thickness of this larger sheet was found to be 16.6 µm. A thinner layer of white precipitate was also observed on the wall of the reactor; this precipitate was composed of aragonite and calcite, and contained an amorphous phase of *ca.* 1%.

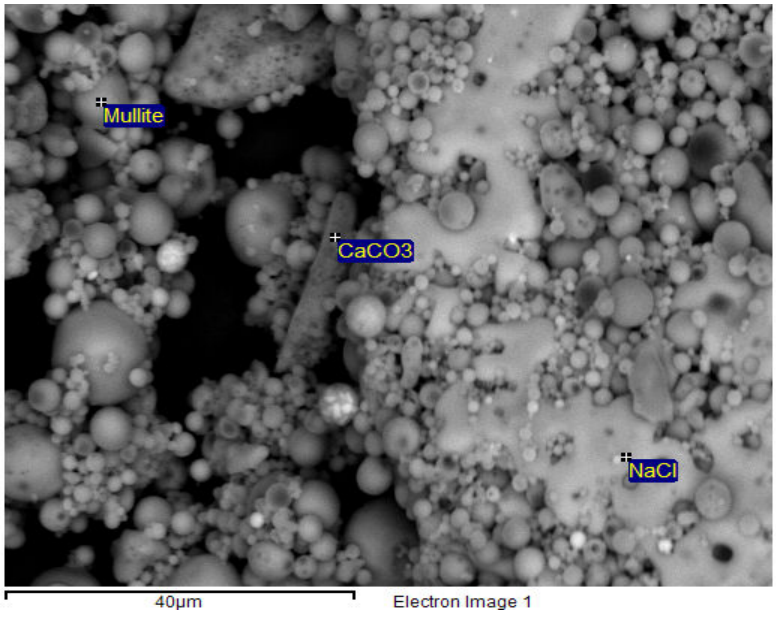

Figure 5.12: SEM micrograph of fly ash treated in CO_2-saturated brine

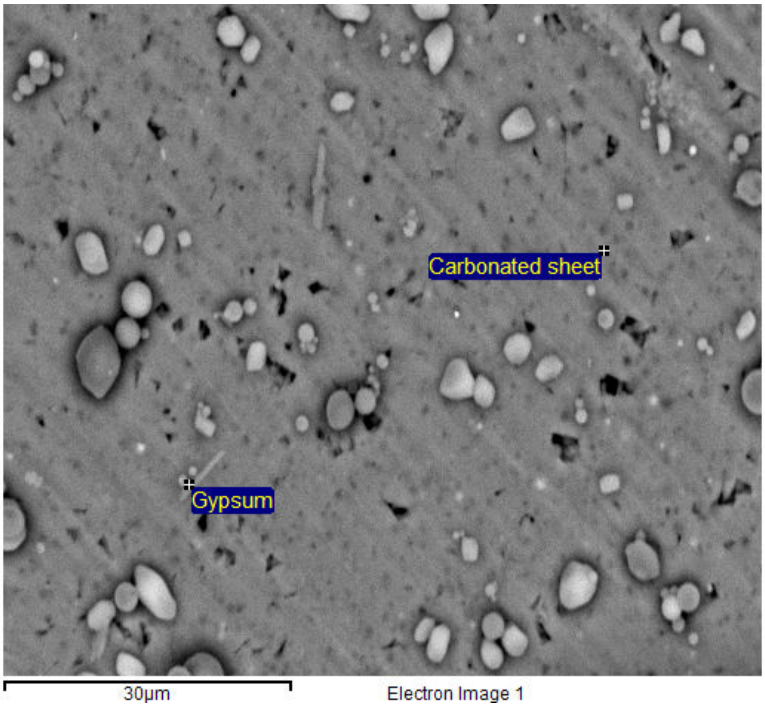

Figure 5.13: SEM micrograph of the surface of carbonated sheet formed from fly ash treated in CO_2-saturated brine

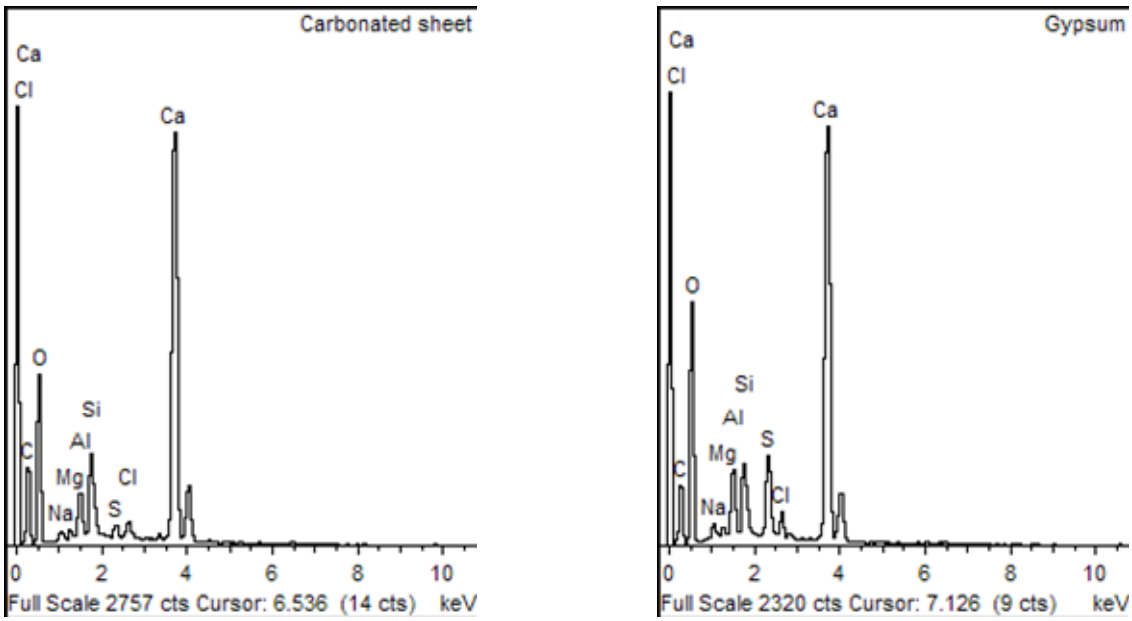

Figure 5.14: Elemental spectra (EDS) of the sheet and needle-like crystal of gypsum. Another crystal of gypsum is shown in the middle top of the micrograph

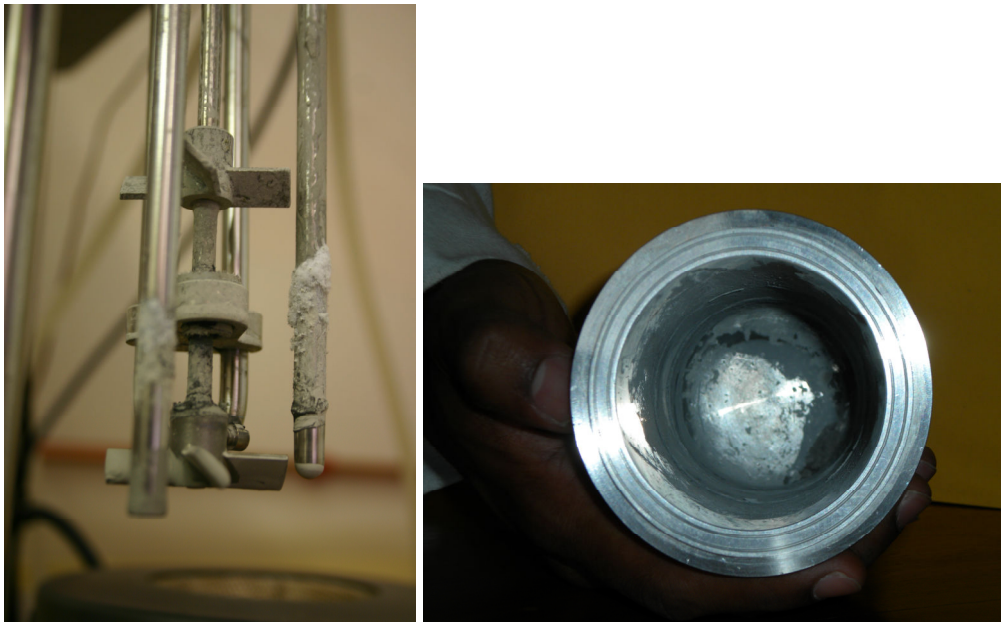

Figure 5.15: Carbonate sheet which formed at and coated the bottom of the high-pressure, high-temperature reactor

After the carbonation experiment some material (carbonates) stick on the walls and on the base of the reactor, while most of the slurry remained in suspension. The red columns in Table 5.15 show the weight percentage (wt %) of the material that was removed from the walls and the base of the reactor. The blue column in the same table shows the amount (in wt %) of the material that remained in suspension throughout the experiment. The material that remained in suspension during the experiment shows very small amounts of carbonate. These carbonates are in the form of aragonite which appears to be favoured under high temperature and pressure conditions with fly ash and brine, as indicated in Table 5.15. Moreover, 1.80 and 1.91 wt% anhydrite was detected and the sulphur is thought to be from CO_2 impurities in a form of SO_2. Between 0.5 and 1.89 g of the sheet material (removed from the base of the reactor) was formed during these experiments. The material that was removed from the base of the reactor shows very low amounts of amorphous phase. This could be caused by the fact that everything that was in suspension poured out of the reactor and only few loose material remained in the reactor. Assuming that only the Ca from the brine reacted to form carbonates – less than 1% of Ca reacted within 2 hr.

Table 5.15: XRD results of fly ash carbonated in brine

Sample	90 °C/50 bar	90°C/50 bar	90°C/90 bar	90°C/90 bar	90°C/90 bar (base)	90°C/90 bar (base)	90°C/50 bar (wall)	90°C/50 bar (wall)
Amorphous Content in wt%	60.56	51.32	64.91	57.03	1.20	37.31	65.23	68.39
Quartz	8.35	8.72	6.16	8.03	12.24	6.40	6.25	5.93
Mullite	25.96	28.67	27.13	32.75	39.65	21.27	26.31	24.12
Aragonite	0.66	0.81	trace	trace	22.65	20.91	1.01	0.79
Calcite	-	-	trace	-	3.83	1.48	trace	trace
Hydrocalumite	-	-	-	-	2.86	3.76	-	-
Anhydrite	1.80	1.91	-	-	-	-	-	-
Halite	2.68	7.72	1.23	1.87	17.61	8.86	0.78	-
Total	100.01	100	99.43	99.68	100.04	99.99	99.58	99.23

*Blue = material that remained in suspension

*Red = material that stuck on the base and walls of the reactor

5.8 The change in carbon content from untreated fly ash to CO_2 treated fly ash

The change in carbon content was investigated using C&S analysis, Figure 5.16. The pale yellow histograms in Figure 5.16 represent the untreated fly ash with a carbon content of 0.34 % by weight. The dark green is the fly ash samples that were treated with CO_2 in ultra pure water. This material contained about 0.48 wt% of carbon. The bright green was carbonated using brine without Ca, Mg and Fe ions, and sodium bicarbonate, here the carbon content has doubled from the untreated material to 0.61 wt%.

The light blue histograms represent the fly ash that was treated with the brine containing all the salts (section 4.5.3.2) and CO_2 that remained in suspension. This material also has twice the carbon as the untreated fly ash of about 0.68 wt%. The dark blue is the material that remained at the base of the reactor and the purple is the material the walls of the reactor. It was also treated with the brine containing all the salts and CO_2. These carbonated samples show a significant increase in carbon content of about 1.49 wt% for materials from the walls and 2.88 wt% for the materials taken from the base of the reactor.

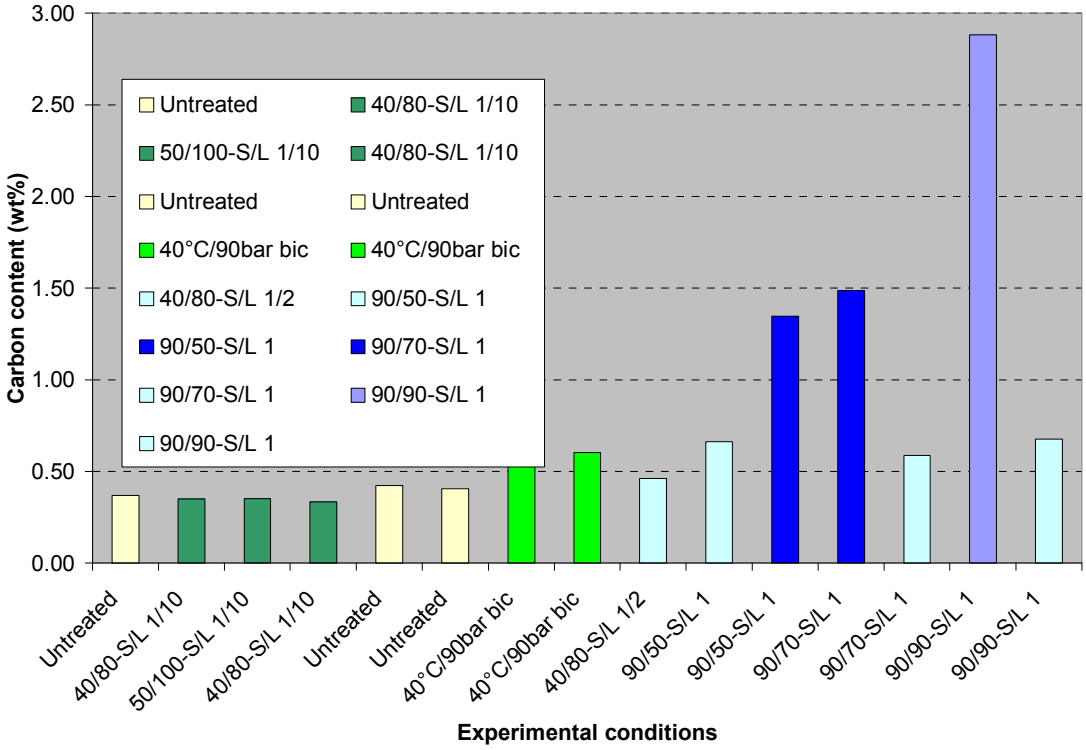

Figure 5.16: The difference in fly ash carbon content for different experimental conditions

5.9 Simulated in-*situ* Carbonation and sandstone characterization

Two sandstone samples from Outeniqua basin (Figure 5.17) were obtained from the PASA core library to conduct CO_2 flooding test and to investigate whether carbonated fly ash can be used to seal rock fractures.

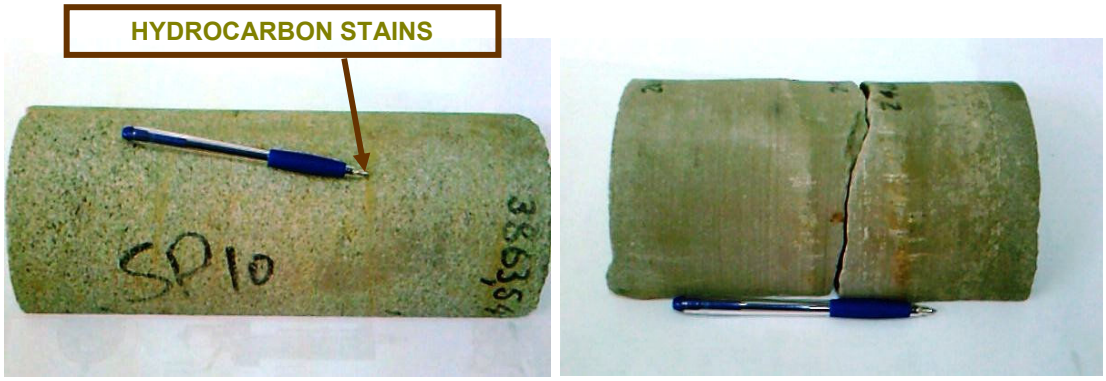

Figure 5.17: Sandstone samples from Outeniqua basin

The mineralogy of these sandstone samples was investigated using a petrographic microscope and by XRD (Table 5.16). Sample AE1 is a medium grained sample which is predominantly composed of quartz and feldspars grains and less chlorite and mica. EAR1 is fine grained sandstone with very high amounts of quartz grains, and considerably less calcite (1.78% vol.) and mica (0.69% vol.).

Table 5.16: XRD analyses of the sandstones

Sample	Calcite	Microcline	Plagioclase	Quartz	Mica	Chlorite
AE1	-	10.4	5.86	75.04	3.5	5.18
EAR1	1.78	trace	0.61	95.96	0.69	-

5.10 Petrography of the sandstone

5.10.1 AE1 Sandstone

AE1 is a sandstone from the Bredasdorp sub-basin. It is a poorly sorted, medium grained rock see Figure 5.18. It is composed mainly of quartz and large very angular feldspar grains (Figure 5.19). Quartz grains are rather rounded, show occasional pressure dissolution and overgrowths that fully occupies the pore space. Rock fragments i.e. siltstone, shale and crystalline rock fragments as well as some mafic components thought to be a pyroxene are present. Sedimentary matrix, calcium carbonate cement and irregular, interstitial mica altered to chlorite are common (Figure 5.20). The quartz grains contained in this rock are better rounded than the feldspar grains are thus interpreted as more proximal since they are also often larger than the quartz grains. Therefore the rock can be seen as bimodal sediment. The rock displays no microscopically visible porosity and evidences features of long diagenetic history and even perhaps metamorphism (low grade), making it a poor reservoir rock and a poor aquifer.

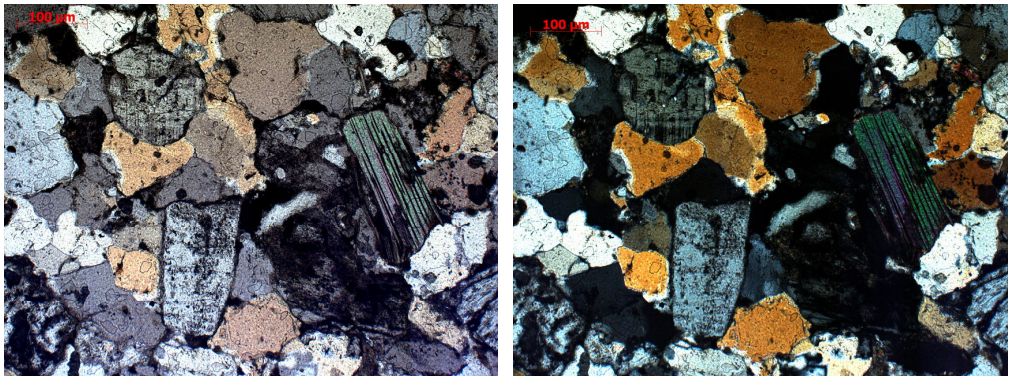

Figure 5.18: Poorly sorted sandstone with very angular feldspar grains from different source than the better rounded quartz grains. The round grain in the upper left half of the micrograph is a microcline. The section is slightly too thick and displays therefore high interference colours. Right picture is under crossed polars.

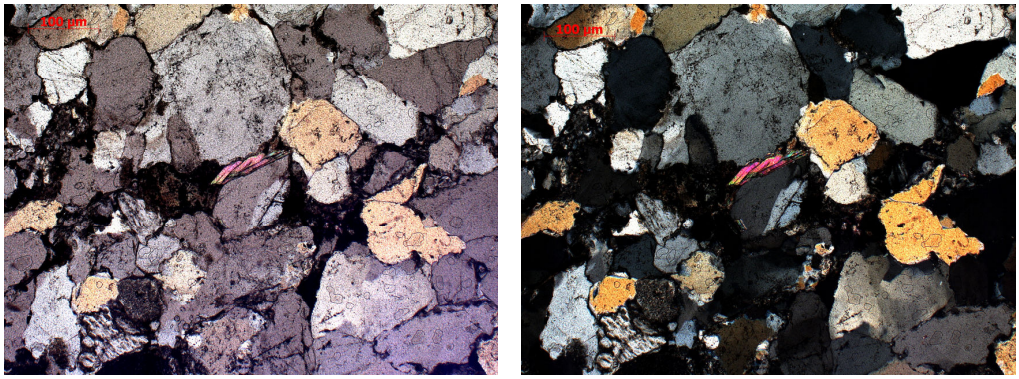

Figure 5.19: Large feldspar grains and sub-round quartz grains with mica fragments (center)

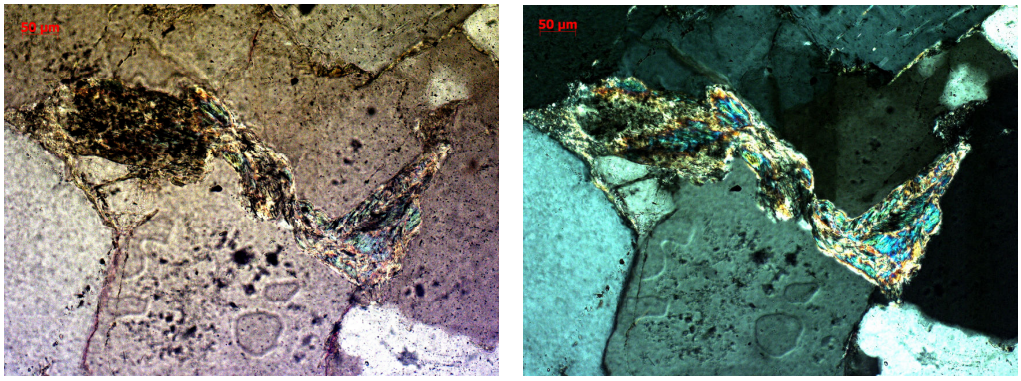

Figure 5.20: Mica and chlorite (anomalous interference colours), squeezed within quartz grains all pictures above show lack of visible porosity in the sandstone

5.10.2 EAR1 Sandstone

EAR1 is a well sorted, fine grained sandstone (Figure 5.21) composed mainly of quartz and digenetic glauconite grains (Figure 5.22). It also consists of small amounts of feldspar and displays a weak quartz overgrowth. It is relatively rich in matrix and poorer in diagenetic calcite (less than 1%). Few zircon grains evidence a crystalline source of this rock (Figure 5.23). This rock has been strongly compacted, displays a grains supported texture and shows pressure dissolution along grain boundaries (Figure 5.24). It is therefore of very low, non visible porosity, and of very low permeability and actually not suitable as a reservoir rock.

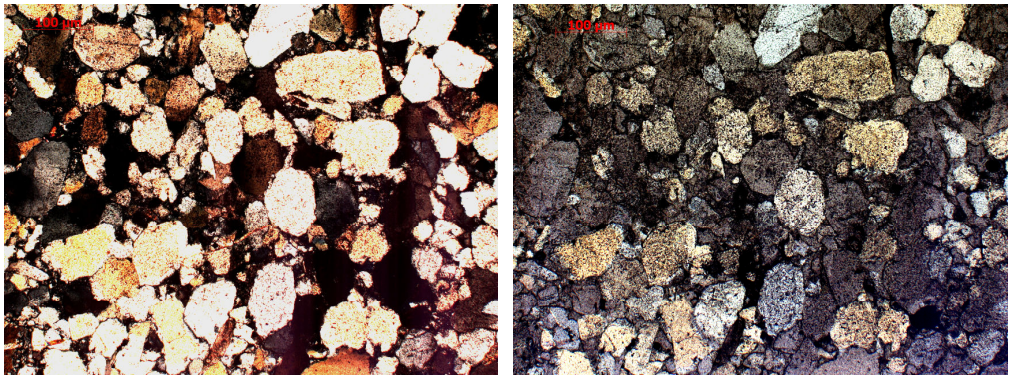

Figure 5.21: Well sorted sandstone with rounded quartz grains of similar size

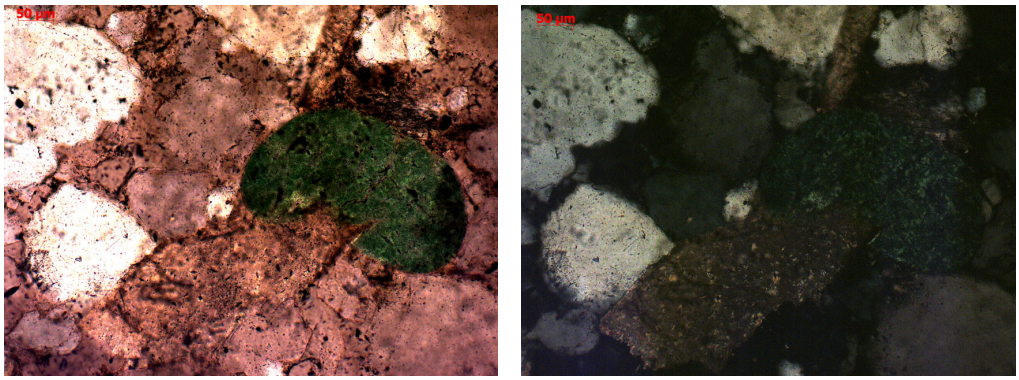

Figure 5.22: Digenetic glauconite grain, evidence for marine sediments in an upwelling shelf facies

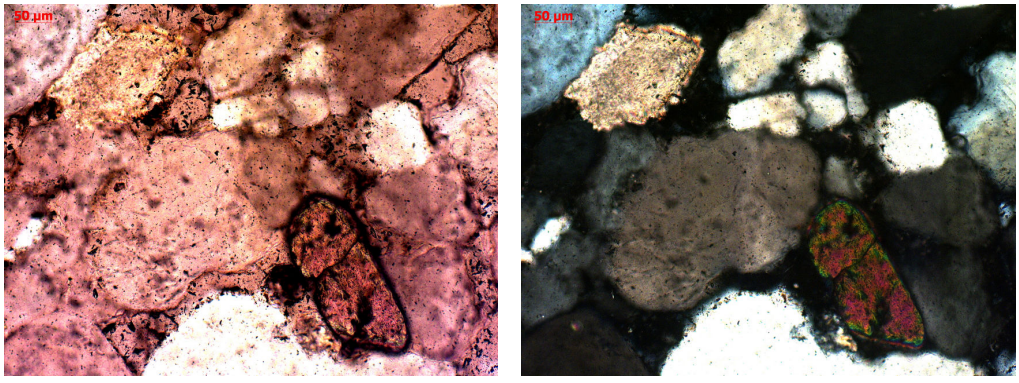

Figure 5.23: Detrital Zircon grain (high relief, lower right part of the picture) and diagenetic calcite grain (higher relief than quartz but lower than zircon, upper left part of the picture). The quartz grain between the zircon and the calcite displays quartz overgrowth. The abundant fluid inclusion traces in this grain continue across the grain boundaries into the overgrowth and evidence a metamorphic overprint of the rock.

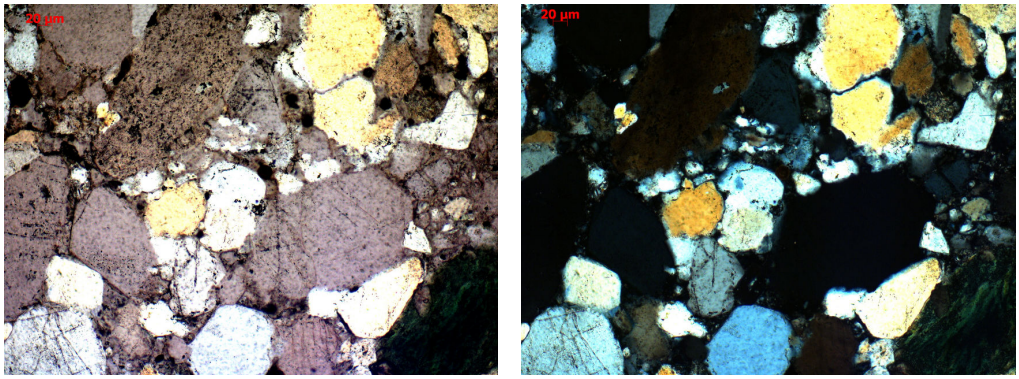

Figure 5.24: Evidence of pressure dissolution in quartz grains (sutured grain boundaries, interlocked in each other), the dissolved SiO_2 precipitated in the interstitial space blocking and filling the pores.

CHAPTER SIX
CONCLUSIONS AND RECOMMENDATIONS

6.1 Conclusion

Within deep saline formations (below 800 meters), CO_2 is in a supercritical state since its critical point lies at 30.98ºC and 73.8 bar (Span et al., 1996). Currently there is no literature available on aqueous carbonation of coal-combustion fly ash in brine waters under supercritical conditions. A clear understanding of aqueous carbonation of fly ash under these conditions is essential if it is to be considered for the purpose of sealing fractures in saline reservoirs. Other materials were also considered but fly ash was regarded as the best for this application because it is available in large quantities, has a favourable rheology, and is available at low cost. Fly ash easily adjusts the pH to favour carbonation. This was observed when fly ash was leached with ultra pure water at room temperature when the pH was above 11 and above 8 when brine was used. In addition, its fine particles (<45 μm) may easily be injected together with fluids into rock fractures and will not require milling before the injection.

The envisaged and desired scenario is that upon injection of fly ash into rock fractures, a back pressure will be created by the fly ash particles which should clog the pores. This should prevent CO_2 from migrating beyond the reservoir confinement. The fly ash will then subsequently react with the CO_2 plume to form a carbonated mineral slurry curtain, which will permanently seal the fracture until the CO_2 is converted into a carbonate mineral, 100s to 1000s of years later.

During this study, it was confirmed that saline formation brine can contribute to the conversion of CO_2 into mineral carbonates, more so, if the pH is above 8 and if there is a large amount of CO_2 dissolved in solution. This is exemplified by the result discussed in section 5.3 where the increase in CO_2 dissolution in brine led to an increase in calcite production by a factor of six within two hours. However, the kinetic mechanisms are still a limiting factor since 100% Ca conversion could not be reached and only about 62% of calcium in solution was converted into carbonates. The 100% conversion of calcium ions into carbonates could possibly be reached by extending the duration of the experiment.

The carbonation of fly ash in ultra-pure water was not successful during the short periods of experiment time. This was thought to be caused by:

- pH which might not have been high enough (pH<8)
- Ca ions were not available in solution
- Kinetic mechanisms were not fast enough for the carbonation to occur within two hours
- Or very little CO_2 dissolved in solution

Experiments were designed that will address these factors separately and that will provide its impact on carbonation. In order to understand the effect of the pH on carbonation; the pH was measured before and after the reactions, since pH could not be monitored during the experiment. The pH factor was not a limiting factor because the pH before the experiment was about 11 and after the experiment it varied between 8 and 10 (Table 5.13).

The question regarding the availability of calcium ions in solution was addressed by the leaching experiments (Tables 5.5 and 5.6). The results presented in these tables show that there is at least 5% by weight calcium ions available in solution. Then, kinetic mechanisms were considered: the experiments with shorter duration showed no evidence of carbonation, was detected by XRD analyses or by the carbon analyser (Tables 5.11, 5.12 and Figure 5.14). However, extending the experiment time resulted in the formation of about 1.78% wt. of calcite during a seven day long experiment. Therefore, it was concluded the carbonation reactions have very slow kinetic mechanisms particularly if there is less CO_2 available in solution.

It was observed by the Albany Research Center (O'Connor et al, 2000) that the dissolution of CO_2 in brine can be improved by the addition of sodium bicarbonate. This phenomenon was proven correct by keeping the experimental conditions the same but adding either sodium bicarbonate or CO_2 gas. The addition of sodium bicarbonate resulted in the formation of carbonates (Table 5.14) without the presence of calcium ions in the brine. Therefore, all the calcium that reacted to form carbonates were from the fly ash.

In addition, an experiment involving brine (containing all salts, section 4.4) was performed with fly ash. This experiment resulted in the formation of aragonite and was the only experiment where aragonite was formed. Aragonite formed on the base and on the walls of the reactor, which was a common observation.

Saline formation brines can form stable carbonates within a short time and the reaction can be improved by improving CO_2 dissolution in brine. The carbonation of fly ash can be enhanced by increasing the CO_2 in solution. Therefore, the two limiting parameters are the rate of the carbonation reaction and the low amount of CO_2 dissolved in the brine.

6.2 Recommendations

- A 100% calcium conversion could not be reached within two hours. Therefore, the period at which the calcium conversion takes place needs to be investigated using CO_2 gas and sodium bicarbonate. The investigation needs to be performed for at least three hours or until 100% calcium is converted into carbonates, whilst keeping the experimental conditions the same.

- It was not possible to carry out the investigation of the effects of supercritical CO_2/brine mixtures on the porosity and permeability of sandstone cores under pressures representative of a depth of 800-2000 m in the presence and absence of fly ash. Therefore, it will be valuable to investigate the flooding of the sandstones by CO_2 in long term tests.

REFERENCES

Angeli, M., Soldal, M., Skurtveit, E., Aker, E. (2009). Experimental percolation of supercritical CO_2 through a caprock. Energy Procedia 1, 3351-3358.

Ash Resource (2012). http://www.ash.co.za, accessed in March 2012.

Bachu, S., (2008). CO_2 storage in geological media: Role, means, status and barriers to deployment, Progress in Energy and Combustion Science, 34, 254–273

Bachu, S., Gunter, W.D., (2004). Acid–gas injection in the Alberta basin, Canada: a CO_2 storage experience, 233. Geol. Soc. Spec. Publ., pp. 225–234

Bachu, S., (2003). Screening and ranking of sedimentary basins for sequestration of CO_2 in geological media in response to climate change. Environmental Geology, 44, 277 – 289.

Bachu, S. and Bonijoly, D. and Bradshaw, J. and Burruss, R. and Holloway, S. and Christensen, N.P. and Mathiassen, O.M., (2007). CO_2 storage capacity estimation: methodology and gaps, International Journal of Greenhouse Gas Control, 1, 430-43.

Blencoe, J.G., Palmer, D.A., Anovitz, L.M., Beard, J.S., (2004). Carbonation of Metal Silicates for Long-Term CO_2 Sequestration. Patent application WO 2004/094043.

Broad, D.S., Jungslanger, E.H.A., and Roux J., (2006) Offshore Mesozoic basins. In: Johnson, M.R., Anhaeusser, C.R. and Thomas, R.J. (Eds.), The Geology of South Africa, Geological Society of South Africa, Johannesburg/Council for Geoscience, Pretoria, 553-571

Busch, A., Alles, S., Gensterblum, Y., Prinz, D., Dewhurst, D.N., Raven, M.D., Stanjek, H., Krooss, B.M., (2008). Carbon dioxide storage potential of shales. Int. J. Greenhouse Gas Contr. 2, 297-308.

Court, B., Celia, M.A., Nordbotten, J.M., Ellio, T.R., (2011). Active and integrated management of water resources throughout CO_2 capture and sequestration operations, Energy Procedia, 4, 4221–4229

Cloete, M. (2010). Atlas on geological storage of carbon dioxide in South Africa. Council for Geoscience, Pretoria, South Africa, pp. 59.

Cloete M., Haddon I.G. & Strachan L.K.C. (2007). TOR for the exploration of geological reservoirs suitable for CO2 storage in South Africa. Unpublished report, Council for Geoscience.

CCSP-H1 (U.S. Climate Change Science Program), (2006). Methane as a Greenhouse Gas, Fact Sheet, January 2006.

CSLF (Carbon Sequestration Leadership Forum), (2011). CO_2 Transportation – Is it Safe and Reliable, inFocus Carbon Capture and Storage, obtained from www.cslforum.org on 24 December 2011.

Dlugokencky, E.J., L. Bruhwiler, K.A. White, J.W.C., Emmons, L.K., Novelli, P.C., Montzka, S.A., Masarie, P.M. Lang, Crotwell, A.M., J.B. Miller, and Gatti, L.V., (2009). Atmospheric methane levels off: Temporary pause or new steady state?, Geophysical Research Letters, 36, L 18803.

Dlugokencky, E.J., S. Houweling, L. Bruhwiler, K.A. Masarie, P.M. Lang, J.B. Miller, and P.P.Tans, (2003). Atmospheric methane levels off: Temporary pause or new steady state?, Geophysical Research Letters, 30(19), 1992.

DeConto, R.M., Pollard, D., Wilson, P.A., Palike, H., Lear, C.H. Pagani, M., (2008). Thresholds for Cenozoic bipolar glaciation, Nature 455, 652-656.

di Norcia, V., (2008). Global Warming is Man-Made: Key Points in the 2007 Fourth Report of the International Panel on Climate Change, Hard Like Water – Ethics In Business, obtained from http://dinorcia.net/GloblWarmgIPCCReportSummary.pdf on 5 September 2011

Doucet F.J., (2011). Scoping Study on Carbon Mineralization Technologies, Report No CGS-2011-007

Doucet F.J., (2008). Carbon dioxide sequestration by industrial mineral carbonation: Evolution of industrial alkaline waste material and their leachates – A South Africa perspective. Annual Progress Report No 2008-0039, Council for Geoscience, pp 39 (restricted access)

Eberhard, A., (2011). The Future of South African Coal: Market, Investment, and Policy Challenges, Working Paper #100 January 2011

Engelbrecht, A., Hietkamp, S., Scholes, B and Golding, A., (2004). The Potential for Sequestration of Carbon Dioxide in South Africa, CSIR and Department of Minerals and Energy 86DD/HT339.

EAR (Eskom Annual Report), (2010). http://financialresults.co.za/2010/eskom_ar2010/gb_env_perf.htm (accessed on 8 March 2011).

EIA (U.S. Energy Information Administration), (2008). In, http://www.ucsusa.org/global_warming/science_and_impacts/science/each-countrys-share-of-co2.html, (accessed on 8 March 2011).

Gevers T., W., (1941). Carbon Dioxide Springs and Exhalations in Northern Pondoland and Alfred County, Natal Geological Society of South Afrca, 233-301

Hay W. W., (2011). Can human force a return to a Cretaceous Climate, Sedimentary geology, 235, 5-26.

Huijgens, J.J., Comans, R.J., (2006). Carbonation of steel slag for CO_2 sequestration: leaching of products and reaction mechanisms. Environ. Sci. Technol. 40, 2790-2796.

Huijgens, J.J., Comans, R.J., (2004). Carbon dioxide sequestration by mineral carbonation, Literature review update 2003-2004, Energy Research Center of Netherlands.

ICCS, (2009). Introduction to Carbon Capture and Storage workshop, Glenhove Conference Center, Rosebank, 28 September 2009

IEAGHG (International Energy Agency GHG), (2010). Greenhouse News, Issue100, December 2010, p 1-14.

IEA (International Energy Agency), (2010). Publications 9 rue de la Fédération, 75739 Paris Cedex 15 Printed in France by Corlet, October 2010

IEAGHG, (2008). Novel Approaches to Improving the Performance of Carbon Dioxide Capture Technical Report Number: 2008/10, September 2008

IEAGHG, (2006). Natural release of CO_2, Report 45

IEAGHG, (2005). Greenhouse Issues, June 2005, Number 78

IPCC (Intergovernmental Panel on Climate Change), (2005). Special Report on Carbon Dioxide Capture and Storage. Prepared by Working Group III of the Intergovernmental Panel on Climate Change [Metz, B., O. Davidson, H. C. de Coninck, M. Loos, and L. A. Meyer (eds.)]. Cambridge University Press, Cambridge, United Kingdom and New York, NY, USA, 3, 107, 181 and 197 pp.

IPCC, 2007. Climate Change 2007: Working Group I: The Physical Science Basis, http://www.ipcc.ch/publications_and_data/ar4/wg1/en/ch2s2-2.html, accessed in 12 June 2012

Johnson, J.W., Nitao,J.J., Steefel,C.I., (2002). Fundamental elememnts of geologic CO_2 sequestration in saline aquifers, Fuel Chemistry Division Preprints, 47 (1), 41

Kaszuba, J.P., Janecky, D.R., Snow, M.G., (2003). Carbon dioxide reaction processes in a model brine aquifer at 200ºC and 200 bar: implications for geologic sequestration of carbon. Appl. Geochem. 18, 1065-1080.

Kaldi, J G and Gibson-Poole C M., (20080. Storage Capacity Estimation, Site Selection and Characterization for CO_2 Storage Projects, March 2008, CO2CRC Report No: RPT08-1001

Kaszuba, John P., Janecky, David R., & Snow, Marjorie G. (2005). Experimental evaluation of mixed fluid reactions between supercritical carbon dioxide and NaCl brine: Relevance to the integrity of a geologic carbon repository. Chemical Geology, 217(3-4), 277-293.

Kruger, R.A, (2010). The pozzolanic reactivity of Class F fly ash, Lecture notes held at Council for Geoscience, February 2010.

Kruger, R.A, and Krueger, J.E., (2005). Historical development of coal ash utilisation in South Africa,

Kruger J.E., (2003). South African fly ash: A cement extender, The South African Coal Ash Association, February 2003

Kruger, R.A, (1997). Fly ash beneficiation in South Africa: creating new opportunities in the market-place Fuel Vol. 76, No. 8, pp. 777-779

Liu Q and Maroto-Valer M. M., (2010). Investigation of the pH effect of a typical host rock and buffer solution on CO_2 sequestration in synthetic brines, Fuel Processing Technology 19 1321-1329

Lu, P., Fu, Q., Seyfried Jr, W.E., Hereford, A., Zhu, C., (2010). Navajo Sandstone-brine-CO_2 interaction: implications for geological carbon sequestration. Environ. Earth Sci. DOI 10.1007/s12665-010-0501-y.

Lu, C., Shik Han, W., Si-Yong Lee, McPherson, B.J., Lichtner, P.C., (2009). Effects of density and mutual solubility of a CO_2–brine system on CO_2 storage in geological formations: ‘‘Warm” vs. ‘‘cold” formations, Advances in Water Resources, 32, 1685–1702

Michael, K., Golab,A., Shulakova, V., Ennis-King, J., Allinson, G., Sharma, S., Aiken, T., (2010). Geological storage of CO_2 in saline aquifers – A review of the experience from existing storage operations, International Journal of Greenhouse Gas Control, 4, 659-667

NETL (National Energy Technology Laboratory), (2008). Geologic sequestration , A national plan for making science-based decision, Factsheet 8.08

Montez-Hernandez, G., Perez-Lopez, R. Renard, F., Nieto, J.M., Charlet, L., (2009). Mineral sequestration of CO_2 by aqueous carbonation of coal-combustion fly ash. J. Hazard. Mat. 161, 1347-1354.

NASA (National Aeronautics and Space Administration), (2005). Methane's Impacts On Climate Change May Be Twice Previous Estimates. ScienceDaily. Retrieved November 10, 2011, from http://www.sciencedaily.com /releases/2005/07/050718214744.htm, (accessed on 14 November 2011).

Nduagu E., Zevenhoven R. (2010) Production of magnesium hydroxide from magnesium silicate for the purpose of CO_2 mineralisation or increasing ocean alkalinity: Effect of reaction parameters. 3rd International Conference on Accelerated Carbonation for Environmental and Materials Engineering, Turku, Finland, pp 31-40.

O'Connor, W.K., D.C. Dahlin, D.N. Nilsen, G.E. Rush, R..P. Walters and P.C. Turner, (2000). CO_2 Storage in Solid Form: A Study of Direct Mineral Carbonation, DOE/ARC-2000-011

O'Connor, W.K., Rush, G.E, (2005). Applications of mineral carbonation to geological sequestration of CO_2. DOE/ARC, Report number 2005-010.

Pirajino, F., (1992). Hydrothermal mineral deposits: Principles and fundament Concept for the exploration geologist, Springer-Verlag

Price, P.N., Oldenburg, C.M., (2009). The consequences of failure should be considered in siting geologic carbon sequestration projects, International Journal of Greenhouse Gas Control, 3, 658-663

Torróntegui, M.D. (2010) Assessing the mineral carbonation science and technology. MSc thesis, ETHZurich, Switzerland, pp. 51.

Saikia,N., Kato, S., Kojima, T., (2006). Compositions and leaching behaviours of combustion residues, Fuel 85, 264–271

Seifritz W., (1990). "CO_2 disposal by means of silicates," Nature 345, 486.

Schaef, H.F., and McGrail, B.P., (2005). Direct measurements of pH and dissolved CO_2 in H_2O-CO_2 brine mixture to supercritical conditions, Greenhouse Gas Control Technology, Volume II, 2169-2173.

Soong, Y., D.L. Fauth, B.H. Howard, J.R. Jones, D.K. Harrison, A.L. Goodman, M.L. Gray, E.A. Frommell, (2006). CO_2 sequestration with brine solution and fly ashes, Energy Conversion and Management 47, 1676–1685

Span, R., Wagner, W., (1996). Journal of Physical and Chemical Reference Data, 1996, 25, p.1509.

Stevens, S. H., J. M. Pearce, A. A. J. Rigg, (2001). Natural Analogs for Geologic Storage of CO_2: An Integrated Global Research Program, First National Conference on Carbon Sequestration U.S. Department of Energy National Energy Technology Laboratory May 15-17, 2001 Washington, D.C.

Sipilä, J., S. Teir and R. Zevenhoven, (2008). Carbon dioxide sequestration by mineral carbonation Literature review update 2005–2007, Report 2008-1

Teir, S., (2008). Fixation of carbon dioxide by producing carbonates from minerals and steelmaking slags, Doctoral Dissertation, Helsinki University of Technology Faculty of Engineering and Architecture Department of Energy Technology

Viljoen J.H.A. Stapelberg F.D.J. and Cloete M. (2010). Technical report on geological storage of carbon dioxide in South Africa, Council for Geoscience.

WMO (World Meteorological Organization), (2011). Greenhouse Gas bulletin, No.7.

WMO (World Meteorological Organization), (2010). Greenhouse Gas bulletin, No.6.

WMO (World Meteorological Organization), (2009). Greenhouse Gas bulletin, No.5.

WMO (World Meteorological Organization), (2006). Greenhouse Gas bulletin, No.1.

WWF (World Wildlife Fund), (2011). South Africa's low carbon development plan, Climate-country Brief, Chris Marais / WWF-Canon, November 2011